

A new look for residential hybrid systems

A PV-battery-electrolyser-fuel cell power system
for a neighbourhood in the Netherlands

by

Sergino A. Vis

to obtain the degree of Master of Science
at the Delft University of Technology,
to be defended publicly on Wednesday August 25, 2021 at 10:00 AM.

Student number:	4271718	
Thesis committee:	Prof. dr. A. Smets,	TU Delft, supervisor
	dr. P. Manganiello,	TU Delft
	dr. ir. A. Shekhar,	TU Delft
	T. de Vrijer,	TU Delft

Preface

Welcome to my thesis report "A new look for residential hybrid systems", which is based on a model of a PV-batteries-electrolyser-fuel cell power system. This thesis was written as a part of my graduation project for my master's degree from the Sustainable Energy Technology department of Delft University of Technology.

Moving from a small island in the Caribbean to the Netherlands was a big leap in my life. Looking back that I have achieved my bachelor degree in Aerospace Engineering and now finishing my master degree in Sustainable Energy Technology seems like a wild adventure. Living through ongoing Covid-19 pandemic and doing my whole master's thesis from home was not what I expected for my graduation project. But in hard and extremely challenging times the only thing you can do is keep moving forward, one step at a time.

I would like to thank my supervisors, Arno Smets and Thierry de Vrijer, for their guidance and support during my graduation project. Also, I would like to thank Megan Atkins who helped me understand the modelling program.

I would also like to thank Mirna Loefstop, Aveline Figaroa and Karel Vis for their daily support and motivation. With-out them the lockdown periods and isolation would have made this trajectory much more difficult.

I would like to end this preface By using the following quote that was very relevant to this model;

"There is no silver bullet. There are always options and the options have consequences." - Ben Horowitz

*Sergino A. Vis
Aruba, August 2021*

Abstract

With the rise of various renewable energy sources, comes the possibility for combining the different type of sources together to balance their shortcomings. The goal is to find a renewable energy system that can be reliable year-round and be accessible for everyone. This research tries to model such a system.

A model of a grid-tied PV-battery-electrolyser-fuel cell power system, which is based on a continuation of a series of master thesis projects, was expanded to include a neighbourhood with a fully electrical load or a combination of electrical and hydrogen loads. This model was developed to answer the following question.

What is the techno-economic feasibility of a grid-tied PV-battery-electrolyser-fuel cell power system for a household area in the Netherlands which is either fully electrical or hydrogen integrated?

This hybrid system is simulated by using the graphical interface program TRNSYS. The system size of the PV, batteries, electrolyser, fuel cell and hydrogen gas storage tank are optimised by the GenOpt, an add-on for TRNSYS. The optimisation algorithm will try to find the lowest levelised cost of energy (LCOE) while keeping the system self-sufficiency ratio (SSR) around 1 [%]. This will mean that only 1 [%] of the load is allowed to be extracted from the grid.

The simulation is based on a neighbourhood that consists of 630 houses located in Pijnacker Netherlands. All houses will be equipped with a roof mounted solar PV system with centralised batteries, electrolyser, fuel cell and a hydrogen storage tank. If needed the model can be extended to include a small solar park next to the neighbourhood.

The model will simulate two scenarios for a simulation time of one year, the first being that the neighbourhood is fully electrical and the second for a neighbourhood with integrated hydrogen gas in its consumption. The cases that are simulated can be seen in table 1, which have different load profiles. The first one is the base, with only the electrical load demand of houses. Then the load profile will be extended by adding vehicle to the neighbourhood, including the heat demand of the house. These additional load profiles will either be electrical energy based for the fully electrical scenario or hydrogen gas based for the integrated hydrogen scenario.

To estimate the economic development of this hybrid system, a price projection of PV, battery, electrolyser, fuel cell, hydrogen heating, heat pumps and inverters components were determined for the years 2020, 2030, 2040 and 2050. a, the cases will all be simulated for these years. The economic analysis will be over the systems lifetime, which is 25 years.

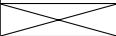
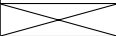
Before the cases were simulated the model undertook a sensitivity analysis. From this resulted that the simulation start time can be moved from the 1st of January to the 2nd of March to relief the storage tank of getting depleted at the start of the simulation. A battery discharge constraint was lifted and this led the batteries to provide more energy. A forecasting method was applied to the system that effectively reduced the electrolyser on/off cycles by 60 [%], which increased the lifetime of the electrolyser component.

From a technical feasibility analysis of the cases, it resulted that the integrated hydrogen scenario was not technical feasible with the PV system (roof mounted with the PV park) of this model. All the integrated hydrogen scenario cases resulted in a depleted hydrogen storage tank, which forced the system to buy the hydrogen demand externally. The system will rely on an external source more than the allowed 1 [%] (hydrogen gas SSR \gg 1 [%]) of the load demand. From the fully electrical scenario the 2020 C-E_{V+H} case resulted not be technical feasible with a SSR value of 2.1 [%]. All the other cases were technical feasible.

From an economic and cost perspective, the cases resulted that the LCOE reduced with the years. The lowest LCOE value found was for the C-E_{Base} case, which reduced from 0.44 [€/KWh] in 2020 to 0.21 [€/KWh] in 2050. The cost breakdown of the cases resulted in the PV system and the storage tank to be the most expensive components of this system. Due to the fact that the C-H_{2H} case had to buy a significant amount of hydrogen from an external source, this became a significant expensive cost of the system.

Comparing the two scenarios resulted that the integrated hydrogen scenario system sizes were smaller, but this is an effect of the system being more eager to buy hydrogen gas then to expand the hydrogen production components. As both scenarios had different SSR values of their respected energy demands, a conclusion of which scenario is more beneficial will be inadequate.

Table 1: The scenarios with their corresponding load profiles can be seen in this table. Their abbreviations are given in this table.

Scenario	Load profile		Base	Vehicle	Heat demand	Vehicle + heat demand
	Years					
Fully electrical	2020		C-E _{Base}	C-E _V	C-E _H	C-E _{V+H}
	2030		C-E _{Base}	C-E _V	C-E _H	C-E _{V+H}
	2040		C-E _{Base}	C-E _V	C-E _H	C-E _{V+H}
	2050		C-E _{Base}	C-E _V	C-E _H	C-E _{V+H}
Integrated hydrogen	2020			C-H _{2V}	C-H _{2H}	C-H _{2V+H}
	2030			C-H _{2V}	C-H _{2H}	C-H _{2V+H}
	2040			C-H _{2V}	C-H _{2H}	C-H _{2V+H}
	2050			C-H _{2V}	C-H _{2H}	C-H _{2V+H}

Contents

Abstract	ii
List of Figures	vi
List of Tables	viii
1 Introduction	1
1.1 The new look of energy	1
1.2 Why this hybrid system?	1
1.3 Research goal	3
1.4 Thesis outline	4
2 The future hydrogen town model	5
2.1 Programming tool: TRNSYS	5
2.2 Location	5
2.3 System overview & components	6
2.3.1 Solar power hybrid system	6
2.3.2 Component description	6
2.3.3 Master controller	8
2.4 Economics	10
2.5 System performance	10
3 Current and future trends	12
3.1 Household demand trends	12
3.2 Electricity and hydrogen price trends	13
3.3 System components trends	14
3.3.1 Solar panels	15
3.3.2 Batteries	15
3.3.3 Electrolyser	15
3.3.4 Fuel cell	16
3.3.5 Hydrogen heating components	17
3.3.6 Heat pumps	17
3.3.7 Inverter	19
4 System optimisation	20
4.1 Optimisation algorithm	20
4.1.1 Objective function	20
4.1.2 Optimisation variables	21
4.2 Scenarios	22
4.2.1 The fully electrical scenario	22
4.2.2 The integrated hydrogen scenario	23
5 Result & discussion	24
5.1 Sensitivity analysis on the model	24
5.1.1 SSR penalty function	24
5.1.2 Simulation start time	25
5.1.3 Constrains on the batteries charge cycle	25
5.1.4 Electrolyser cycle regulator	25
5.2 An analysis of the cases	27
5.2.1 Technical feasibility analysis	27
5.2.2 Economical and cost analysis	31
5.2.3 The reliance on hydrogen storage	36

- 5.2.4 The cost differences between the low and high projected prices 37
- 6 Conclusion & recommendations 40
 - 6.1 Conclusion 40
 - 6.2 Recommendations for future work 42
- A Components price trend curves 43
- B Optimisation results 47

List of Figures

1.1	Schematic diagram of the hybrid system from the paper of Tamarzians(2019)[17].	3
2.1	Schematic diagram of the hybrid system represented in green box and the secondary system represented in the orange box.	6
2.2	The flow diagram of the model, which indicates how the power distribution in the model takes place.	9
3.1	The hydrogen consumption profile for one week of the neighbourhood demands.	13
3.2	The cost of PV system is plotted against time. The best case represent the most optimal scenario for PV integration and the normal case is the scenario stays as business as usual[51].	15
3.3	The lithium-ion batteries system cost is plotted with time. This plot was modified to illustrate the trend lines clearly, the unmodified data points plot can be seen in appendix A figure A.1. The points in the legend corresponds with the source in the bibliography[52–64].	16
3.4	The electrolyser cost is plotted with time. This plot was modified to illustrate the trend lines clearly, the unmodified data points plot can be seen in appendix A figure A.2. The points in the legend corresponds with the source in the bibliography[8, 53–56, 65–70].	16
3.5	The fuel cell cost plotted with time. This plot was modified to illustrate the trend lines clearly, the unmodified data points plot can be seen in appendix A figure A.3. The points in the legend corresponds with the source in the bibliography[52, 56, 65, 72–74].	17
3.6	The cost of a hydrogen boiler plotted with time. To get the boiler unit price for this model the cost has to multiplied by 40. This plot was modified to illustrate the trend lines clearly, the unmodified data points plot can be seen in appendix A figure A.4. The points in the legend corresponds with the source in the bibliography[76–79].	18
3.7	The heat pump system cost plotted with time. To get the heat pump unit price for this model the cost has to be multiplied by 7.9. This plot was modified to illustrate the trend lines clearly, the unmodified data points plot can be seen in appendix A figure ???. The points in the legend corresponds with the source in the bibliography[52, 54, 65, 78, 80–92].	18
3.8	The inverter unit cost plotted with time. This plot was modified to illustrate the trend lines clearly, the unmodified data points plot can be seen in appendix A figure A.6. The points in the legend corresponds with the source in the bibliography[93–101].	19
5.1	The SSR results are illustrated for the fully electrical scenario with a SSR weight constant of 60. The years represent the results of the model if the system was constructed in set year.	28
5.2	The SSR results are illustrated for the attained results of integrated hydrogen scenario. The years represent the results of the model if the system was constructed in set year. The big plot presents the electrical SSR_E values, which is the percentage of electrical energy that the system takes from the grid. The small plot represents the hydrogen SSR_{H_2} values, which is the percentage of hydrogen gas demand that was taken from an external source. The optimisation for the case C- H_{2V} were stopped after the PSO section, as mid optimisation it was noticed that the system has no hydrogen storage function. The results for C- H_{2V+H} was not searched for, as the case C- H_{2V} already had no hydrogen storage function.	29
5.3	On the left axis the SOC of the hydrogen storage tank can be estimated over the simulation time of one year, the SOC is represented by the blue line. On the right axis the volume flow rate can be estimated for the fuel cell and hydrogen boiler. These are dependent on the electrical demand and heat demand of the neighbourhood. The plot presents the data of C- H_{2H} case of year 2020.	29

5.4	On the left axis the SOC of the hydrogen storage tank can be estimated for the first week of the simulation, the SOC is represented by the blue line. On the right axis the volume flow rate can be estimated for the fuel cell, HV and electrolyser. The flow rate of the fuel cell is dependent on the electrical demand and the amount of stored hydrogen gas. The flow rate of the HV is dependent on an average private vehicle usage. The flow rate of the electrolyser is dependent on surplus power. The plot presents the data of C-H _{2V} of year 2050.	30
5.5	The LCOE results are illustrated for the fully electrical scenario. The years represent the results of the model if the system was constructed in set year.	31
5.6	The left plot presents the size difference of the PV system for every case of the fully electrical scenario. The differences are estimated to year 2020. The right plot presents the price of the PV system and cost difference. The legends data correspond to both plots.	32
5.7	The demand and generation of electricity are presented here for a summer and winter week. The data are taken from the results of the 2020 C-E _V case. The legend data correspond to both plots.	33
5.8	The total cost breakdown can be seen with its corresponding components. Every component of the hybrid system can be seen in the legend, while some components are not present in the chart for this case. This chart represents the component cost of the C-E _{Base} case.	34
5.9	The LCOE results are illustrated for the C-H _{2H} case. The years represent the results of the model if the system was constructed in set year.	34
5.10	The total cost breakdown is illustrated for the C-H _{2H} case. Every component of the hybrid system can be seen in the legend, while some components are not present in the chart for this case.	35
5.11	The total cost breakdown is illustrated for both scenarios for the base case with heating. The integrated hydrogen scenario is presented by the bar plot with H ₂ on top of it and the fully electrical scenario is presented by EL. Every component of the hybrid system can be seen in the legend, while some components are not present in the chart for this case.	36
5.12	The stacked bar plot represents the fraction of the load demand that is provided by the given component. This fraction is estimated for the whole simulation period of one year. This plot presents the results from the C-E _{Base} case.	37
5.13	The stacked bar plot represents the fraction of the load demand that is provided by the given component. The bar plot with the lighter colours represents the fractions of C-H _{2H} case and the bar plot with the darker colours represents C-E _H . This fraction is estimated for the whole simulation period of one year.	38
5.14	The total cost breakdown of C-E _{V+H} case is presented for both low and high projected prices. The results for the low projected price are indicated by the bar plots with Low and the results for the high projected price are indicated by High. Every component of the hybrid system can be seen in the legend.	38
A.1	The lithium-ion batteries system cost is plotted with time. The points in the legend corresponds with the source in the bibliography[52, 53, 55–61, 63, 64].	43
A.2	The Electrolyser cost is plotted with time. The points in the legend corresponds with the source in the bibliography[8, 53–56, 65–70].	44
A.3	The fuel cell cost plotted with time. The points in the legend corresponds with the source in the bibliography[52, 56, 65, 72–74].	44
A.4	The cost of a hydrogen boiler plotted with time. To get the boiler unit price for this model the cost has to multiplied by 40. This plot was modified to illustrate the trend lines clearly, the unmodified data points plot can be seen in appendix A figure A.3. The points in the legend corresponds with the source in the bibliography[76–79].	45
A.5	The heat pump system cost plotted with time. To get the heat pump unit price for this model the cost has to be multiplied by 7.9. The points in the legend corresponds with the source in the bibliography[52, 54, 65, 78, 80–92].	45
A.6	The inverter unit cost plotted with time. The points in the legend corresponds with the source in the bibliography[93–101].	46

List of Tables

1	The scenarios with their corresponding load profiles can be seen in this table. Their abbreviations are given in this table.	iii
2.1	Location parameters of Ackerswoude in the Netherlands.	6
2.2	Panasonic HIT N340 PV module parameters[24].	7
2.3	The batteries characteristic used in the model[26][27].	7
2.4	The Inverter parameters used in the model.	8
3.1	The investment, maintenance, replacement, fuel and lifetime of the components for this hybrid system are presented here. Some of these parameters stayed the same as for the previous work[18].	14
3.2	The component investment cost over the years. This is only for the low price trends.	14
4.1	The search-space and step sizes that are used for the optimisation algorithm.	22
4.2	The scenarios with their corresponding load profiles can be seen in this table. These will shape the cases that are researched. Their abbreviations are given in this table and will be further used in the paper to refer to them. The crossed out boxes were not researched because the base load profile does not change between the two scenarios.	22
5.1	The LCOE and the corresponding SSR value results from the optimisation of the various SET-SSR and weight constant. The first number is the LCOE and the second italic number is the SSR value. The green boxes represent the lowest value for each SET-SSR value.	24
5.2	The change in cycling of the electrolyser with the time step forecasting method. The corresponding LCOE and SSR value are the result of the optimisation with the forecast time steps.	26
5.3	In this table the cases which are technical feasible and not feasible are presented. The cases which are presented in green are technical feasible, the cases which are presented in red are not feasible. A discussion on why they are feasible or not will be in presented in subsection 5.2.1. The cases with an asterisk have a PV park attached to their system.	27
6.1	The scenarios with their corresponding load profiles can be seen in this table. Their abbreviations are given in this table.	40
B.1	The results of the sizing for the hybrid system for each case in the fully electrical neighborhood scenario.	48
B.2	The results of some parameters of the hybrid system for each case in the fully electrical neighborhood scenario. These results are related to the low prices components trend.	49
B.3	The results of the sizing for the hybrid system for each case in the integrated hydrogen neighborhood scenario.	50
B.4	The results of some parameters of the hybrid system for each case in the fully electrical neighborhood scenario. These results are related to the low prices components trend. For this scenario it was chosen to leave out the results of C-H _{2V} and C-H _{2V+H} as both did not produce any feasible data.	51

1

Introduction

1.1. The new look of energy

In recent decades there has been a surge in the variety of alternative energy source. In 2020 the renewable energy capacity grew by 45 [%] from 2019, which was the highest year-on-year increase in the last two decades. This growth is led by 134 [GW] solar photovoltaics(PV) net capacity added in 2020[1]. As the implementation of alternative energy source is being accelerated, more research are being done on various types of alternative energy grew. The search is to find a year-round reliable energy system that will emit little to no green house gas(GHG) emissions and be accessible to every one. Achieving these goals will mean that the conventional energy systems which society is used to will have to change. As any other complicated systemic issue, there is no 'silver bullet solution' to provide energy to the masses. Therefore, the combination of various energy sources or hybrid energy systems is an interesting research subject.

1.2. Why this hybrid system?

PV is a mature technology and becoming a household name with various PV systems emerging around the globe. There is a fast growing market for PV with the cumulative PV installation between 2010 to 2019 having a compound annual growth rate of 35 [%][2]. PV system are now providing the cheapest electricity for various installation around the world[3]. Also, PV systems are projected to reach a cumulative capacity higher than 1 [TW] by 2023[4].

This growth is also expected to be sustained in the coming decades with adequate regulatory frame work, reducing capital expenditures and stretching the efficiency together with reliability[5].

The compactness and relatively low maintenance of PV panels makes it an energy source that can be installed on residential houses. This will mean that energy can be generated decentralized and very close to the consumer.

A PV system brings with a constant production/consumption mismatch, as the irradiance on the system will vary in the day which will vary the production. This makes periods where there are excess energy and others periods of deficit. To better utilise the produced energy from a PV system a storage system will need to be added, this will then store the excess energy to be used in a period where there is a deficit.

One common energy storage system are batteries. As of 2018, batteries are the third biggest global storage system in operational capacity[6]. Batteries have the highest round trip efficiency for a storage system with no start up time[7]. This made batteries one of the most reliable system for daily storage. But batteries do struggle with long term storage because of their high self-discharge rate.

To relief the long term storage shortfall of batteries, storing energy as hydrogen gas is a solution. This power-to-gas concept will convert the excess electrical energy to hydrogen gas by a water electrolyser, the hydrogen gas will then be stored. When needed, the hydrogen gas will be converted back to electrical energy with a fuel cell. The hydrogen gas can also be utilised in the transport sector, heating sector or manufacturing industries. Water electrolysis technology is wildly used and already operational in large-scale industrial applications [8]. This technology was not largely applied yet with renewable energy sources, as their intermittent behaviour

limits the electrolyser efficiency and reduces the gas purity.

As of now fuel cells are not yet widely applied, which makes the technology relatively expensive. The recent application of fuel cell are focused on the transport sector with the developments of hydrogen powered vehicle(HV). For the residential sector, in some Asian countries fuel cell combined heat and power(FC-CHP) units are being applied in homes. For Japan the residential FC-CHP unit will play a vital role on reducing their GHG, as the Japan's road map estimates 5.3 million unit being installed by 2030[9].

Conventionally, gas will be stored in a gas tank, but due the low volumetric energy density the hydrogen gas will need to be compressed. The hydrogen gas can be compressed to a high pressure of 700 [bars], which bring extra safety measurements, complexity and cost to storing hydrogen gas.

By combining these components a hybrid system can be constructed that will generate electrical energy with a PV system, store electrical energy short term with batteries and have the potential to store energy long term by converting it to hydrogen. Such system has been researched in variety of locations and scale. In most works the system is designed for one building and being a fully stand-alone system.

A stand-alone hybrid system for an African household was modelled by Lagorse et al.(2008). The goal was to find the most cost effective system size. The system which consisted of PV-battery-electrolyser-fuel cell power system obtained the lowest levelised cost of energy(LCOE) of 0.645 [€/KWh][10].

A stand-alone PV-battery-electrolyser-fuel cell power system to meet the demand of an academic research building located in central India was modelled by Singh et al.(2017). This paper presented a techno-economic feasibility analysis of the hybrid system. The lowest cost of energy obtained with a 0 [%] capacity shortage was 0.203 [\$/KWh][11].

The paper by Das et al.(2017) presented a stand-alone PV-battery-electrolyser-fuel cell power system for a longhouse of 50 families in eastern Malaysia. The goal of paper was to compare the system to the conventional diesel based electrical system. It resulted that the PV-battery-electrolyser-fuel cell power system(cost of energy of 0.323 [\$/KWh]) was more economical then the diesel based electrical system(cost of energy of 0.638 [\$/KWh]) [12].

An example of a hybrid system but with a connection to the grid is that of Ghenai et. al(2017). This paper presents a grid-tied PV-battery-electrolyser-fuel cell power system for a university building in the UAE. The LCOE obtained for this hybrid system was 0.071 [\$/KWh] with 28 [%] of the load being provided by the grid[13].

Another grid-tied PV-battery-electrolyser-fuel cell power system was modelled in Isa et al.(2016) paper. This hybrid system will provide a hospital in Malaysia with electricity and heating. The heat demand will be provided by a combined heat and power fuel cell system and a boiler which burns hydrogen gas. This system will also produce hydrogen from reforming natural gas. The lowest LCOE obtained was 0.091 [\$/KWh] with 18 [%] of the demand being met by the grid[14].

As can be noticed most of these system are in a region with high solar irradiance and hot weather. Higher solar irradiance will lead to a smaller PV system size with a smaller levelised cost compared to the same system in a region with lower irradiance. Also the hybrid system that were connected to a grid had around 10 times lower LCOE then the stand alone hybrid systems, but had around a fifth of their demand met by the grid.

When observing this hybrid system on a global scale a paper by Fasihi(2020) modelled a hybrid PV-wind-batteries-electrolyser-gas turbine power system for every location over the whole world. The system will use the renewable production to either provide electricity or hydrogen gas. The gas turbines in this model were hydrogen gas powered and provided electrical power. The model was run for a simulation time of 10 year with time steps of 1 hour. The model will result in a cost-optimised configuration of baseload electricity and baseload hydrogen. This research resulted that the base load electricity can be generated at a LCOE less than 0.119, 0.054, 0.041 and 0.033 [€/KWh] for 2020, 2030, 2040 and 2050, across the best sites. A maximum annual cumulative generation potential of 20000 [TWh] was reached. The base load hydrogen resulted a LCOE of 0.066, 0.048, 0.040 and 0.035 [€/KWh_{H₂}] for 2020, 2030, 2040 and 2050 respectively, with a 20000 [TWh_{H₂}] annual cumulative generation potential. The best result typically came from place which have a high average solar irradiance[15].

This research is a continuation of a series of master thesis projects on the PV-battery-electrolyser-fuel cell power system model designed by the PVMD group[16]. Tamarzians(2019) wrote the first master thesis of the series which presented a model for a stand-alone PV-battery-electrolyser-fuel cell power system for one typical Dutch household, its schematic diagram can be seen in figure 1.1[17]. Thereafter, Atkins(2020) wrote the second master thesis which expanded the model to a grid-tied hybrid system for a neighbourhood in Pijnacker Netherlands[18]. Atkins work found for the de-centralized PV generation scenario for the cases of

smart load management (SLM), heat & electrical and electrical vehicles (EV) a LCOE of 0.848 [€/KWh], 1.295 [€/KWh], 0.841 [€/KWh] respectively. Also the cases had about 1 [%] of the demand met by the grid. Atkins work obtained a higher LCOE than that of the other papers. Therefore, the location where the hybrid system is installed has a noteworthy impact on the LCOE value. Also, for Atkins work the reliance on grid power was at 1 [%] of the load which is lower than the previous grid-tied hybrid system papers. This also effected the higher LCOE values.

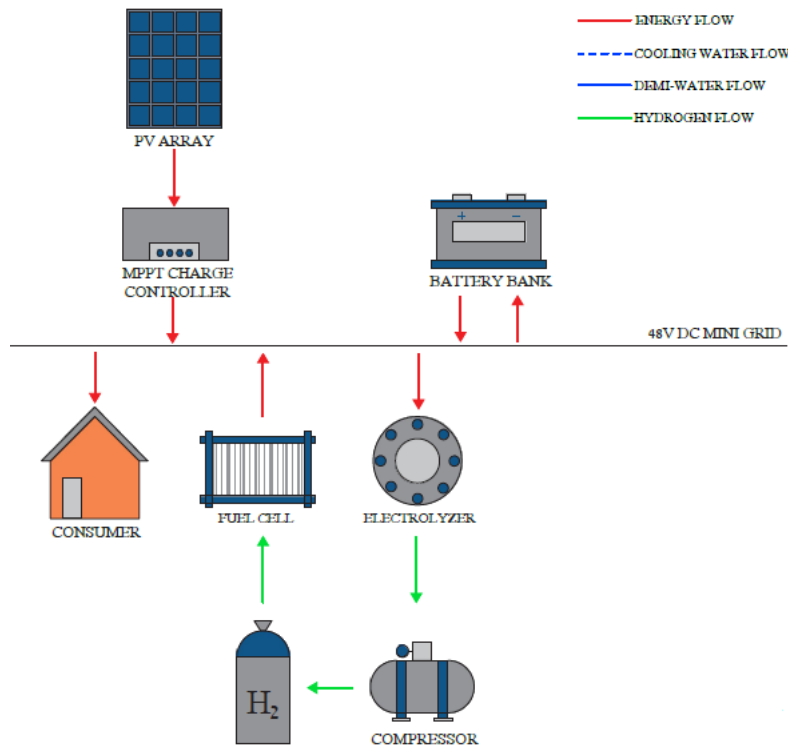


Figure 1.1: Schematic diagram of the hybrid system from the paper of Tamarzians(2019)[17].

This short literature review showed that there is distinctive difference in performance between the hybrid systems in low and high irradiance locations. That most of the research are based on a stand alone system or researched a baseload application. This then raises a question of what is the potential of such hybrid system in a low irradiance location and will it also reach such low LCOE at one point. How does this hybrid system perform in an urban environment, an example being a neighbourhood in the Netherlands. The hybrid system must only be equipped with a PV system to achieve the low irradiance effect. The potential of providing electricity and hydrogen from such hybrid system was only addressed in two papers, these were for the base load and for a hospital building. As electricity and hydrogen gas are being generated by this hybrid systems, the system can easily provide electricity and hydrogen gas to its consumer. Therefore, applying this hybrid system to a neighbourhood which has electrical load and hydrogen load is a possibility.

1.3. Research goal

This thesis project will attempt to elaborate on a grid-tied PV-battery-electrolyser-fuel cell power system which can simulate either a fully electrical neighbourhood or a neighbourhood which has hydrogen integrated. With this neighbourhood laying in a region with low irradiance as the Netherlands brings higher cost. Adding the system cost projection for the foreseen future, an elaboration on the economic development of such system can be visualized.

To encompass the electrical and integrated hydrogen neighbourhoods and systems cost changes, the techno-economic feasibility of such system will be analysed. Therefore, the research question can be stated as:

What is the techno-economic feasibility of a grid-tied PV-battery-electrolyser-fuel cell power system for a household area in the Netherlands which is either fully electrical or hydrogen integrated?

This research question can be answered with the help of these two key questions:

- To what extent does the techno-analysis feasibility vary for a household demand with a vehicle, with heat demand or with both?
- How does the PV-battery-electrolyser-fuel cell power system cost vary between the period of 2020-2050?

To start answering the research questions, first the previous work by Atkins(2020) will have to be elaborated on. As this thesis project is a continuation of Atkins thesis project, the de-centralized PV generation scenario from Atkins work will be further expanded[18]. The cases presented in this research will resemble that of Atkins work with the exception of the load profiles being combined to represent the neighbourhood better. The model will simulate the workings of the hybrid system with the load demands of the houses, EV and heat pump heating; or the load demands of a neighbourhood that has integrated hydrogen. This will include hydrogen demand from a hydrogen heating components and hydrogen powered vehicles(HV).

The development of the cost for the hybrid system will be estimated by estimating a price for every decade between the year 2020 to 2050 for the main components.

1.4. Thesis outline

The thesis is structured in 4 main chapters besides the introduction and conclusion. After this introduction chapter 2 will elaborate on the inner workings of the model. There the location and duration of the simulation will be discussed and a schematic diagram of the hybrid system presented. Also, important components and variables used in this model will be elaborated on.

As the main components of the system will then be clear, an analysis about the prices development of these components will be presented in chapter 3. This will be accompanied by the estimated prices of electrical energy and hydrogen gas. The trends related to the electrical and heat demands will also be presented in chapter 3.

In Chapter 4, the optimisation algorithm that is used to size the hybrid system will be established. The variables that will be optimised and the objective function will be elaborated upon. The chapter will end with the scenarios and cases that will be simulated by the model. This will make it clear which load profile will be used for which case.

Chapter 5 consists of two parts. Part one presents the results from a sensitivity analysis of the model from Atkins work. Part two presents the results of the cases that were presented in chapter 4. This will be done by first starting with a technical feasibility analysis, followed by an economic and cost analysis of the cases. Chapter 5 will end with a discussion about the reliance of the cases on the hydrogen storage and a comparison between the two cost that are predicted from the prices developments. For every analysis in this chapter a comparison will be made between a neighbourhood which are fully electrical or has integrated hydrogen. The thesis will end with a conclusion of the research followed by a recommendation section for future works.

2

The future hydrogen town model

In this chapter the model will be introduced and its key aspects will be elaborated on. The programming tool, location that the simulation is based on and a schematic diagram of the model with all its main components will be presented. The main components will also be discussed, as well as the control diagram. The final section will elaborate on the used economic- and system performance parameters.

2.1. Programming tool: TRNSYS

The model is simulated with the use of a graphical interface program TRNSYS[19]. This software was developed by the University of Wisconsin and specializes in the fields of renewable energy, thermal and electrical simulations. For this project TRNSYS 17 version was used. The simulation studio of TRNSYS is the graphical interface of the model where all the components can be seen. The components can be further modified in Fortran 90 programming language, which one can code in a component of ones choice[20].

The advantage of using TRNSYS is that it uses a 'black box' approach, which means that the user does not have to know detailed knowledge of the components to build a model. The components are linked to each other by inputs and outputs; and TRNSYS comes with a preset library. This approach enables the user to study the behavior of the whole system immediately.

As this project is a continuation of previous PVMD works by Tamarzians(2019) and Atkins(2020), components that were designed by PVMD are used and modified as needed[17][18]. This reduces the 'black box' approach, which increases the certainty that the components fit in the model.

2.2. Location

This model is based on a neighbourhood in the Netherlands located in Ackerswoude Pijnacker-Nootdorp. In Ackerswoude they are building a new neighborhood, which could be retrofitted to accommodate the hybrid system introduced here[21]. 630 houses have been integrated in this model and are assumed to be identical in layout and construction planning. This model will utilise the roof of the houses in the neighbourhood to install the PV systems, which will make use of an area with little other function. A beneficial method for a country like Netherlands which is relatively densely populated. 40% (252 houses) of the houses are in the south south east(SSE) orientation, 58% (366 houses) in the south west west(SWW) orientation and 2% (12 houses) in the south(S) orientation. The solar panel orientation would reflect the orientation of the houses. The houses are built for an average family with only one private vehicle.

Meteorological data

The meteorological data used for this model is the same used as for the previous works[18]. This is the 2017 data from Meteonorm of the Delft region[22]. The location parameters can be seen in table 2.1. For the calculation of the PV power the incident irradiance on the plane of the solar array(PAO) is used. This takes into account beam radiation, diffuse radiation and ground reflected radiation. The method used to determine PAO irradiance is the Perez Sky Diffuse model[23].

Table 2.1: Location parameters of Ackerswoude in the Netherlands.

Parameter	Value
Latitude	52.03 °(North being 0°)
Longitude	4.45°(East being 0°)
Altitude	40°(Horizontal is 0°)
Albedo (snow)	0.7
Albedo (no snow)	0.2

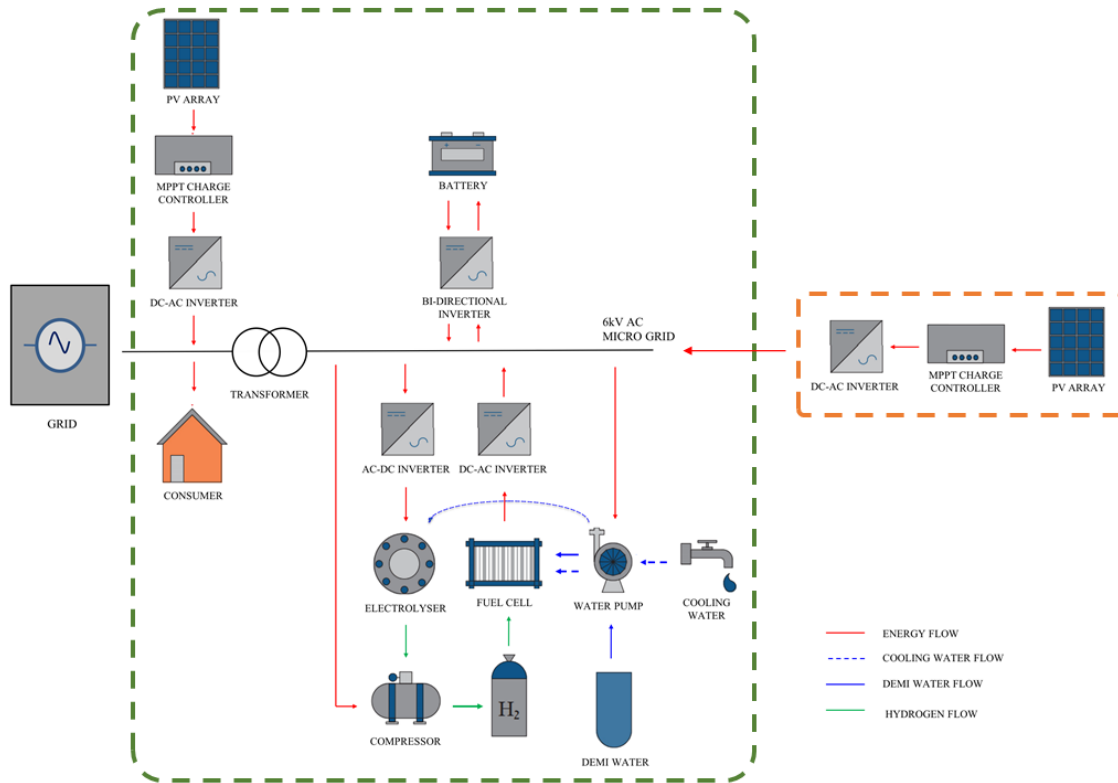


Figure 2.1: Schematic diagram of the hybrid system represented in green box and the secondary system represented in the orange box.

2.3. System overview & components

The system consists of three main elements which are the solar power generation, short term storage and long term storage. The short term storage is achieved with the use of batteries and long term storage with storing hydrogen gas. This system replicates the decentralized PV generation scenario from the previous work[18]. In the next sub-section the system will be illustrated and the components will be defined.

2.3.1. Solar power hybrid system

The System is built on 5 components which are as follows; solar panels, batteries, electrolyser, fuel cell and storage tanks. A schematic diagram of the hybrid system can be seen in figure 2.1. The boxes around the components represent the main system and a secondary system attached in some cases. This is only used when there is a need of more energy production, this will further be elaborated on in section 5.2.1.

2.3.2. Component description

In this subsection every component technology will be described. For the most part the technology and assumption does not vary from Atkins(2020) work, therefore I would like to refer to the previous work to why these decisions were taken[18].

Table 2.2: Panasonic HIT N340 PV module parameters[24].

Parameter	Value	Description
P_{mpp}	340 W	Power at maximum power point
V_{OC}	71.3 V	Open circuit voltage
I_{SC}	6.04 A	Short circuit current
V_{mpp}	59.7 V	Voltage at maximum power point
I_{mmp}	5.7 A	Current at maximum power point
NOMT	44 °C	Normal Operating Module Temperature
$\mu_{V_{oc}}$	-0.235 %/°C	Temperature coefficient open circuit voltage
$\mu_{I_{sc}}$	0.055 %/°C	Temperature coefficient short circuit current
$\mu_{P_{mpp}}$	-0.258 %/°C	Temperature coefficient maximum power point
η_m	20.3 %	Module efficiency
A_m	1.67427 m ²	Area of module
γ	1.5	Ideality factor crystalline silicon

Table 2.3: The batteries characteristic used in the model[26][27].

Parameter	Value	Description
η_{charge}	90 %	Battery charging efficiency
SOC_{min}	20 %	Minimum state of charge
C-rate	0.5	Charging rate

Mono-crystalline solar panels

The solar cell type is mono-crystalline, because these have a higher average efficiency than poly-crystalline solar cells. The array is modeled after Panasonic HIT N340 PV module, a black high powered solar panel[24]. The parameters of the solar panels can be seen in table 2.2.

Lithium-ion batteries

The batteries are centralized for the whole neighborhood, therefore lithium-ion battery type is chosen. As newer project integrate more and more lithium-ion batteries, the increasing capacity of lithium-ion batteries led to declining system cost which drives more integration of lithium-ion[25]. The characteristics of the battery could be seen in table 2.3.

Alkaline electrolyser

An alkaline electrolyser is used in this model as it is the most widely available electrolyser type. The electrolyser component is based on HyProvide Large-Scale Alkaline Electrolyser project by GreenHydrogen with some parameters of PHOEBUS system by Muerer and Ulleberg(1999)[28][29].

PEM fuel cell

The fuel cell in this model is based on Proton Exchange Membrane Fuel(PEM) Cell technology. The fuel cell component is modeled after a design by Amphlett(1995), with some adjustment to model an industrial size fuel cell[30].

Compressed storage tank

The hydrogen gas is stored in a compressed storage tank at maximum allowed pressure of 500 [BAR]. The storage tank is modeled after TRNSYS storage tank component designed by Goetzberger(1993)[31].

Auxiliary components

- **Compressor:** The Compressor is modeled after RIX Model 4VX3BG-65, which reaches the maximum pressure of 500 [bar] at maximum flow rate of 170 [m³/h][32]. The compressor component can be found in TRNSYS component library.
- **Inverter/rectifier:** There are three different inverters in the model, the main difference is between the inverter used for the roof solar arrays and that of the solar park. Both of these inverter parameters can be seen in table 2.4. The third inverter is used for the fuel cell and has an efficiency 97 [%]. A rectifier is used for the electrolyser and the batteries, it is assumed to have a constant efficiency of 93 [%].

Table 2.4: The Inverter parameters used in the model.

Parameter	Roof solar array	Solar park
Inverter	Fronius Primo: 3.8-1 240[34]	SOLECTRIA PVI-75-480[35]
P_{AC0} [W]	3800	75000
P_{DC0} [W]	3911.35	77916.68
V_{DC0} [V]	650	345
P_{S0} [V]	53.25	784
C_0 [W ⁻¹]	$-3.14 \cdot 10^{-6}$	$-3.6 \cdot 10^{-7}$
C_1 [V ⁻¹]	$-3 \cdot 10^{-5}$	$3.89 \cdot 10^{-6}$
C_2 [V ⁻¹]	$-4.8 \cdot 10^{-5}$	$-1.39 \cdot 10^{-5}$
C_3 [V ⁻¹]	$2.76 \cdot 10^{-4}$	$-1.76 \cdot 10^{-3}$

- **Pump:** There are two water pumps in this system, one for cooling the fuel cell and one to feed the electrolyser demineralised(DEMI) water. The water pump component could be found in TRNSYS component library.
- **Heat pump:** The heat pump in the model is based on Rameha Mercuria E heat pump with a capacity of 7.9 [KW]. As this heat pump has a seasonal performance factor of around 4, this would be enough to meet the heat demand for one household[33].
- **Micro-grid:** The components of the system would be directly connected to the local distribution grid in Ackerswoude, this could be presented as a micro grid. This AC micro grid has a voltage level of 6 [KV]. It is also assumed that the cables in between the components will cause a loss of 2 [%].
- **Transformer:** As there is a difference between household voltage (240 [V]) and micro-grid operating voltage (6 [KV]), a transformer is used to facilitate changes in between. This transformer is assumed to have an efficiency of 97 [%].

2.3.3. Master controller

The master controller represent the control mechanism of the system. It does this with the predefined control algorithm for every time step in the run time of the model. The model has a time step of 0.125 hour (7.5 minutes) and simulates for a whole calendar year. The system operation are the following The PV system generates power. The generated power compared to the load demand will determined if there is over- or under-generation. If there is over-generation, the excess energy will be stored in either the batteries or by making hydrogen gas to store in gas tanks. When there is under-generation the deficiency will be met by either the batteries or fuel cell or both. As the micro-grid acts as the intermediate between all the components, there is a local power station with a transformer near all the centralized components.

Flow diagram

The master controller has three operational modes that controls the energy flow in the system. These operational model can be seen figure 2.2 and will be elaborated on further.

Operational mode 1

When the power generated is greater than the load demand, it gives a positive net power flow ($P_{net} > 0$). If the batteries are not fully charged, power will be delivered to the batteries until they are fully charged. If there is excess power ($P_{exc} > 0$) after the maximum charge rate of the batteries was reached and the tank are not full, this excess power will be directed to the electrolyser system to make hydrogen gas. If there is still any excess power after the maximum rated power of the electrolyser, the excess energy would be delivered to the grid system.

Operational mode 2

In this mode the PV generation will be smaller than the load demand, there is under-generation and net power flow is negative ($P_{net} < 0$). If the batteries state of charge(SOC) is above the minimum SOC, the battery will provide the needed power. If there is still a shortage the fuel cell will provide the needed power until the hydrogen tank is empty. If there is still a shortage of power, then the system will take the needed power from the grid. This would be considered as a deficit energy that the system will need.

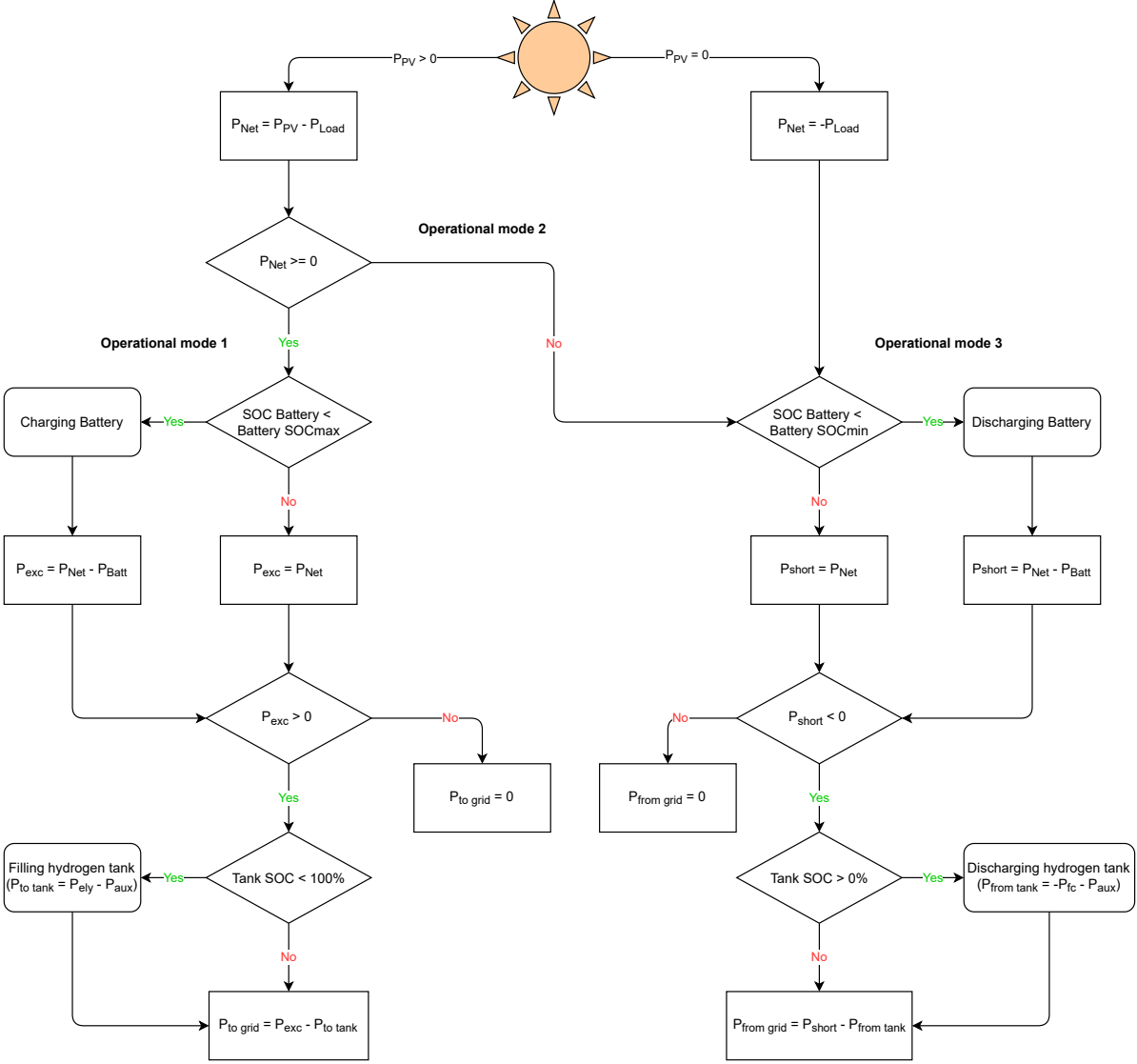


Figure 2.2: The flow diagram of the model, which indicates how the power distribution in the model takes place.

Operational mode 3

In this mode there is no solar power production and the net power flow is negative ($P_{\text{net}} < 0$). The control flow would follow the same route as that of operational mode 2.

2.4. Economics

One of the main metric for this model is LCOE, which will be used to optimise the sizing of the system and give information about the viability of the system. LCOE is defined as can be seen in equation 2.1.

$$\text{LCOE} = \frac{\sum_{n=1}^{k=y} \frac{I_{C_i} + M_{C_i} + R_{C_i} + F_{C_i} - \text{Rev}_i}{(1+r)^y}}{\sum_{n=1}^{k=y} \frac{E_{\text{gen-load}}}{(1+r)^y}} \quad [€/KWh] \quad (2.1)$$

Where the variables are:

- I_{C_i} , investment costs in year i
- M_{C_i} , maintenance costs in year i
- R_{C_i} , replacement costs in year i
- F_{C_i} , fuel costs in year i
- Rev_i , revenue from selling energy in year i
- $E_{\text{gen-load}}$, generated energy delivered to the load
- y, project lifetime
- r, discount rate

The total generated energy that is delivered to the load is defined as seen in equation 2.2. Here P_{gen} is the power provided to the load from the system, excluding the power taken from the grid.

$$E_{\text{gen-load}} = \sum_{i=1}^N P_{\text{gen-load}_i} \Delta t_i \quad (2.2)$$

The project lifetime is set at 25 years, the same as the previous work[18]. The discount rate and the installation cost also did not change, the discount rate is 5% and the installation cost is 10% of the total cost of the system.

2.5. System performance

As the system can extract electricity from the grid, the self-sufficiency ratio(SSR) is introduced to check how much the system is dependent on the grid. The SSR represents the fraction of the load demand that is supplied by the grid, as this becomes bigger the system is more reliant on grid energy. The SSR is defined as could be seen in equation 2.3, where the instantaneous dependence is calculated. The instantaneous dependence is achieved by estimating the SSR value for each time step and then summing it up.

$$\text{SSR}_E = \sum_{i=1}^N \frac{P_{\text{fromgrid}_i}}{(P_{\text{load}_i} + P_{\text{aux}_i})} \cdot 100[\%] \quad (2.3)$$

- i, the time step
- P_{fromgrid_i} , the power taken from the grid at time step i
- P_{load_i} , the load power at time step i
- P_{aux_i} , the auxiliary components power at time step i

For the scenario with integrated hydrogen demand, a SSR value can also be calculated for hydrogen energy. This then estimates how much of the demanded hydrogen is provided by an external source. In the model this will be calculated by using equation 2.4.

$$SSR_{H_2} = \sum_{i=1}^N \frac{m_{\text{from external}_i}}{m_{H_2 \text{ demand}_i}} \cdot 100[\%] \quad (2.4)$$

- i , the time step
- $m_{\text{from external}_i}$, the hydrogen gas mass provided from by an external source at time step i
- $m_{H_2 \text{ demand}_i}$, the hydrogen mass demand of the neighbourhood at time step i

3

Current and future trends

In this chapter the prices of individual components are discussed, as well as their expected development over time. Additionally, trends related to the electrical energy and heat demand are projected. The chapter will be structured in the following order; demand trend, prices of commodities and trend projection of the system components.

3.1. Household demand trends

As households head towards a more sustainable future, the energy efficiency of these households will be an important element. A household that becomes more efficient can demand less energy from this hybrid system while also reducing its electricity bill[36]. In this section the energy demand of the neighborhood with the underlying assumption will be introduced.

Electricity demand

The electrical demand of the houses are the same as the previous work which was build using Load Profile Generator[18][37]. From all the previous load profile presented in the previous work, Smart Load Management(SLM) was chosen for this research[18]. SLM is the demand profile which would be the most financially beneficial for the hybrid system[38].

It was assumed that for every 10 years the average household electricity demand will reduce with 5 [%] or 0.51 [%] every year. This reduction of electrical demand is relatively small compared to that in other works[39]. But by keeping the demand reduction small the electrical demand will not reduce too much by 2050, which can lead to an under-estimated LCOE result by 2050.

Heat demand

The heat demand of the neighbourhood is similar to the previous work[18]. It is assumed that the heat demand will not change significantly in the next couple of decades.

The heat demand for the hydrogen scenario will be provided by hydrogen boilers installed in each house. The hydrogen fuel will be provided from the hydrogen tank in the system. Data sheets of a hydrogen boiler are not widely available, with only a few companies like Remeha providing a design of a boiler specific for hydrogen gas[40]. The modeling of a hydrogen boiler component was skipped as this is not a goal of this research, instead the volumetric flow of hydrogen was calculated. The heating system was assumed to be a closed system and the hydrogen combustion energy will directly feed the heat demand of the house. Therefore, the volumetric flow of hydrogen is estimated by using the heat demand and the lower heating value of hydrogen gas. The relationship can be seen in equation 3.1. The efficiency of a hydrogen boiler was assumed to be 97 [%].

$$\dot{V}_{H_2\text{gas}i} = \frac{Q'_i}{\eta_{H_2\text{boiler}} \cdot LHV_{H_2\text{gas}}} \cdot 3600 \quad (3.1)$$

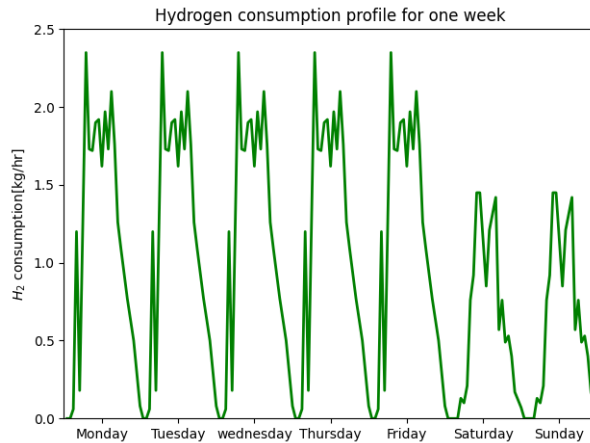


Figure 3.1: The hydrogen consumption profile for one week of the neighbourhood demands.

- $\dot{V}_{H_2\text{gas}i}$, volumetric flow of hydrogen to the boiler at time step i [m^3/hr]
- Q'_i , heat demand from the neighbourhood at time step i [W]
- $\eta_{H_2\text{boiler}}$, hydrogen boiler efficiency of 97 [%]
- $LHV_{H_2\text{gas}}$, lower heating value of hydrogen gas of 10.8 [MJ/m^3] [41]

Transportation

In this model every house will have one private vehicle and will reflect the scenario that has to be simulated. In the electrical scenario all vehicles will be electric and for hydrogen scenario they will be hydrogen powered vehicles.

The EV charging profile is the same as that of the previous work[18]. It is also assumed that every household will be equipped with an EV charging port. The energy that the EV will demand has to be provided by the system.

For the hydrogen powered vehicles a hydrogen consumption profile was constructed by following a hydrogen distribution profile of a hydrogen refueling station in California[42]. This paper presented an average profile for weekdays and weekends, and the data did not specify how many vehicles were charged for this profile. To size the hydrogen consumption profile, first the average annual mileage in 2019 by a passenger vehicle in the Netherlands was estimated to be 12.8 thousand kilometers[43]. A reference hydrogen vehicle is used to find how much hydrogen a passenger vehicle in the Netherlands uses annually. The vehicle used is a Hyundai Nexu which uses 0.84 [kg/H_2] per 100 [km][44]. This led to an annual usage of 107.52 [kg] of hydrogen per vehicle or a total annual hydrogen consumption of 67737.6 [kg] for the neighborhood. To meet the annual hydrogen consumption, it was estimated that the reference profile needs to be scaled with a factor of 7.97. The hydrogen consumption profile can be seen in figure 3.1.

For this research the hydrogen consumption profile will stay the same over the future years.

3.2. Electricity and hydrogen price trends

In this section the trends of the electricity and hydrogen gas prices that are used in the model will be discussed.

Electricity price

In 2020 the average retail price of electricity for a household was 0.16 [$\text{€}/\text{KWh}$][45]. The Rijksoverheid in the Netherlands are going to roll back the "salderen" scheme, which allows consumers that produced more energy than is consumed over the year to be compensated by the energy supplier for their surplus. The price of energy that a consumer is compensated with are 0.206 [$\text{€}/\text{KWh}$] in 2020. The new regulations will set the price for the consumers instantaneous over generation and instantaneous demand the same by 2031, the energy price will be between 0.04 - 0.10 [$\text{€}/\text{KWh}$][46]. Therefore, it was chosen to have an electricity price of

0.08 [€/KWh]. The electricity prices will not change in a simulation run or over all the scenarios.

Hydrogen price

To not make the hydrogen tank depleted over the lifetime of the system, the SOC of the tank at the end of the simulation year should be the same or bigger as that in the beginning of the year. If the SOC of the tank did not meet the initial SOC, the deficit amount of hydrogen will be bought at the end of the year. This is a fail safe mechanism to ensure that the hydrogen system will be sustainable over the project life span.

In the hydrogen scenarios there will be a demand for hydrogen gas that has to be met by the system. If the gas tank is depleted and could not meet the hydrogen demand, the system will need to buy hydrogen from a another supplier.

The price of hydrogen gas is assumed to be 6 [€/kg][47]. For this research it was assumed that the price of hydrogen will stay the same for the future years.

3.3. System components trends

This section will elaborate on the cost of the components and the cost trends of certain components for the future years. Not all the component have a trend analysis, the component parameters that did not change compared to the previous work are illustrated in table 3.1[18].

Table 3.1: The investment, maintenance, replacement, fuel and lifetime of the components for this hybrid system are presented here. Some of these parameters stayed the same as for the previous work[18].

Parameter	Investment cost	Maintenance cost	Replacement cost	Fuel cost	Lifetime
Residential PV	-	3 [%]	-	-	25 years
Lithium-ion Batteries	-	-	100 [%]	-	15 years
Alkaline Electrolyser	-	2.5 [%]	15 [%]	-	60000 [hr]
PEM Fuel Cell	-	6 [%]	50 [%]	-	10000 [hr]
Heat Pumps	-	4 [%]	100 [%]	-	20 years
Hydrogen Boilers	-	4 [%]	100 [%]	-	12 years[48]
Power Inverters	-	3 [%]	100 [%]	-	10 years
Storage tank	950 [€/kg]	1 [%]	-	-	25 years
AC Compressor	€ 130000	6 [%]	100 [%]	-	60000 [hr]
Demi water pump	250 [€/pc]	5 [%]	100 [%]	-	15 years
Cooling water pumps	0.09 [€/m ³]	5 [%]	100 [%]	-	8 years
AC-DC Rectifier	0.22 [€/W]	1 [%]	100 [%]	-	25 years
DC-DC Converter	0.75 [€/W]	-	100 [%]	-	10 years
Gas Dryer	820 [€/pc]	-	8 [%]	-	95 [m ³] (100 [%] RH)
DEMI-Water	-	-	-	30 [€/m ³]	-
Cooling Water	-	-	-	0.93 [€/m ³]	-

The cost trends were investigated by collecting various projections of a technology type. Two trends were identified from the data set, a high price and a low price. The high prices will refer to around an average of the data points. The low prices will refer to the minimum of the data points collected. Most of the 2020 data points reflect the prices openly available at the present day. The investment cost of the components that were analysed can be seen in table 3.2 with their corresponding year.

Table 3.2: The component investment cost over the years. This is only for the low price trends.

Component	Investment cost 2020	Investment cost 2030	Investment cost 2040	Investment cost 2050
Residential PV	1.008 [€/W _p]	0.73 [€/W _p]	0.51 [€/W _p]	0.367 [€/W _p]
Lithium-ion Batteries	0.13 [€/Wh]	0.075 [€/Wh]	0.045 [€/Wh]	0.035 [€/Wh]
Alkaline Electrolyser	0.36 [€/W]	0.21 [€/W]	0.14 [€/W]	0.095 [€/W]
PEM Fuel Cell	1.97 [€/W]	1.1 [€/W]	0.846 [€/W]	0.846 [€/W]
Heat Pumps	3004.5 [€/unit]	2824 [€/unit]	2640 [€/unit]	2464 [€/unit]
Hydrogen Boilers	2062 [€/unit]	1780 [€/unit]	1681.27 [€/unit]	1681.27 [€/unit]
Power Inverters	0.065 [€/W]	0.048 [€/W]	0.032 [€/W]	0.022 [€/W]

3.3.1. Solar panels

In the last decade photovoltaic has had significant development and this development trend is projected to continue[5]. Residential PV capacity could also be further expanded with the proper policy and business models as financial incentives, PV system leasing or Property-assessed clean energy financing[49]. There is also a PV production boost in the recent decade, with China having big role[50].

For this research Fraunhofer-Gesellschaft data was used to estimate the future PV cost trends[2][51]. These trends can be seen in figure 3.2, which includes the cost of a complete PV system. In the Fraunhofer(2015) report various scenarios were presented with different levels of market penetration[51]. This gave a range of what the prices can be per year. The lowest prices and the median were chosen for the lowest and high prices scenario.

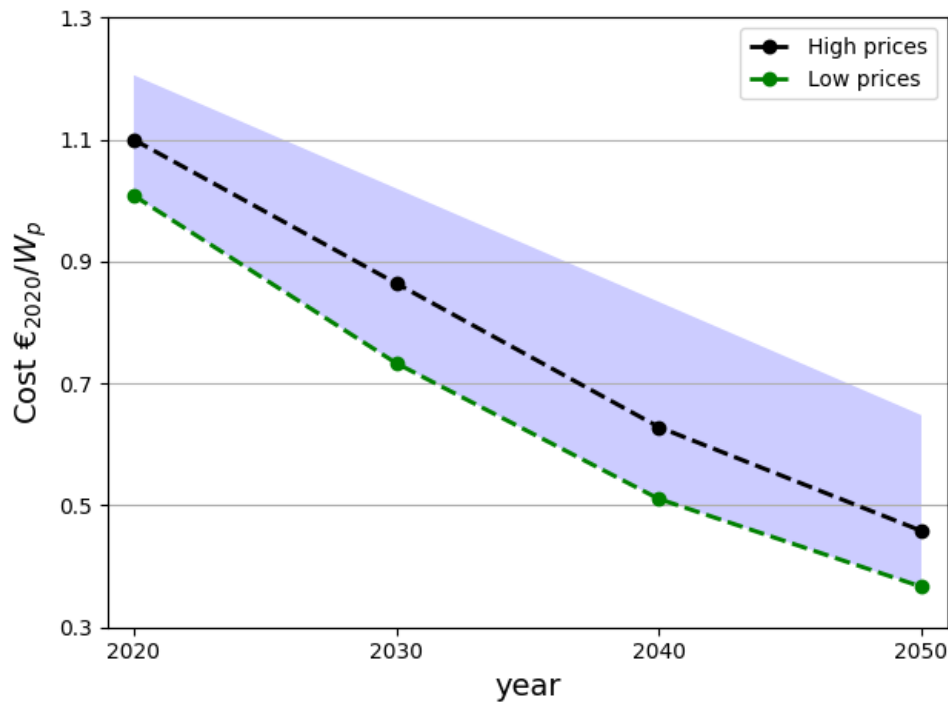


Figure 3.2: The cost of PV system is plotted against time. The best case represent the most optimal scenario for PV integration and the normal case is the scenario stays as business as usual[51].

3.3.2. Batteries

For the batteries a data set consisting of various cost projections was gathered from various sources and papers. All of these include the whole cost of a lithium battery storage system. The data points and the trends could be seen in figure 3.3. From the trend lines it could be seen that between the first two decades there is a steep reduction. The trend for the normal case reduces by 50 [%] and the best case trend reduce by around 42 [%]. This trend can already be seen as lithium batteries usage and capacity has significantly increased in the last years[25].

3.3.3. Electrolyser

The data points and the trends could be seen in figure 3.4, which include the whole electrolyser system cost. Two technology type were used in this data set, alkaline technology and polymer electrolyte membrane (PEM) electrolyser.

There is significant cost reduction for the best case trend as the price will reduce between 2020 and 2030 by around 42 [%]. Alkaline electrolyser have been functional for many years now ,but using it for energy storage is still not common.

hydrogen gas for power and heat production[71]. Therefore, the data consists of some residential PEM fuel cell costs and it is assumed to be scaled up to make it utility scale. The trends of the fuel cell cost could be seen in figure 3.5, which include the whole system cost.

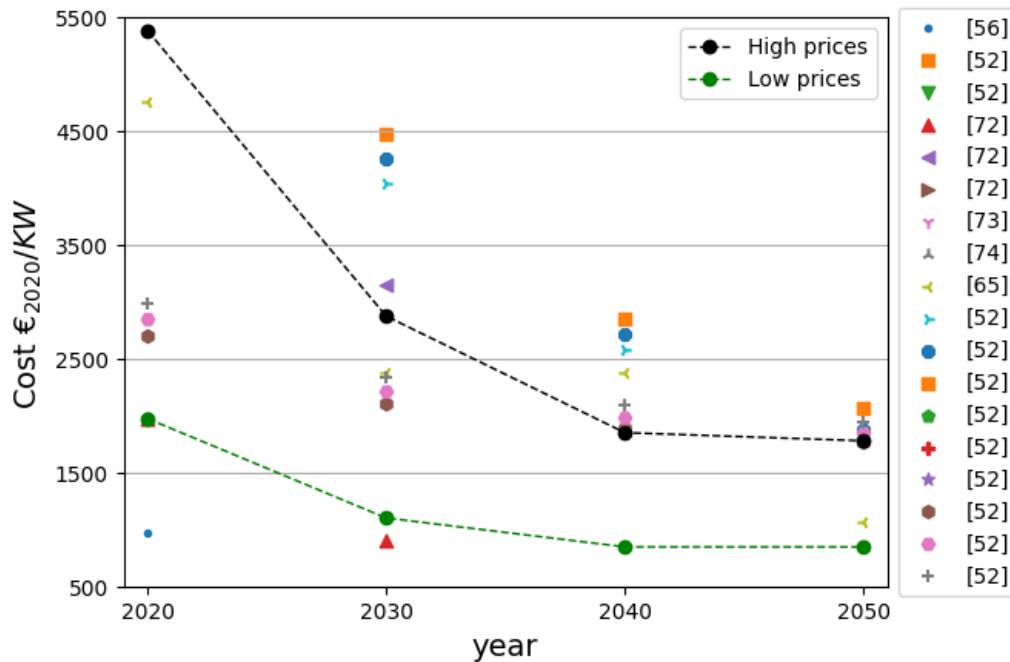


Figure 3.5: The fuel cell cost plotted with time. This plot was modified to illustrate the trend lines clearly, the unmodified data points plot can be seen in appendix A figure A.3. The points in the legend corresponds with the source in the bibliography[52, 56, 65, 72–74].

3.3.5. Hydrogen heating components

For the integrated hydrogen scenario, the home heating system is a boiler that burns hydrogen gas. This technology is still in an early phase and there are no cost projections performed on this topic. It is believed that a hydrogen boiler prices will not vary much from a natural gas boiler[75]. Therefore, projected cost data for a natural gas boiler was used. As a natural gas boiler is a very mature technology and is widely used already, the projected cost will not decrease by much. The trends for the hydrogen heating components could be seen in figure 3.6, which include the cost of the boiler alone. In the model the boiler was assumed to have a nominal power of 40 [KW], which than gave a unit price for each house.

3.3.6. Heat pumps

There are various types of heat pumps, with the air-to-air heat pump being the most known and cheapest. But for this data set various types of heat pumps were considered. The trend could be seen in figure 3.7, which includes the whole system cost of the heat pump system. With the heat pump capacity being 7.9 [KW], a unit cost was calculated for each house.

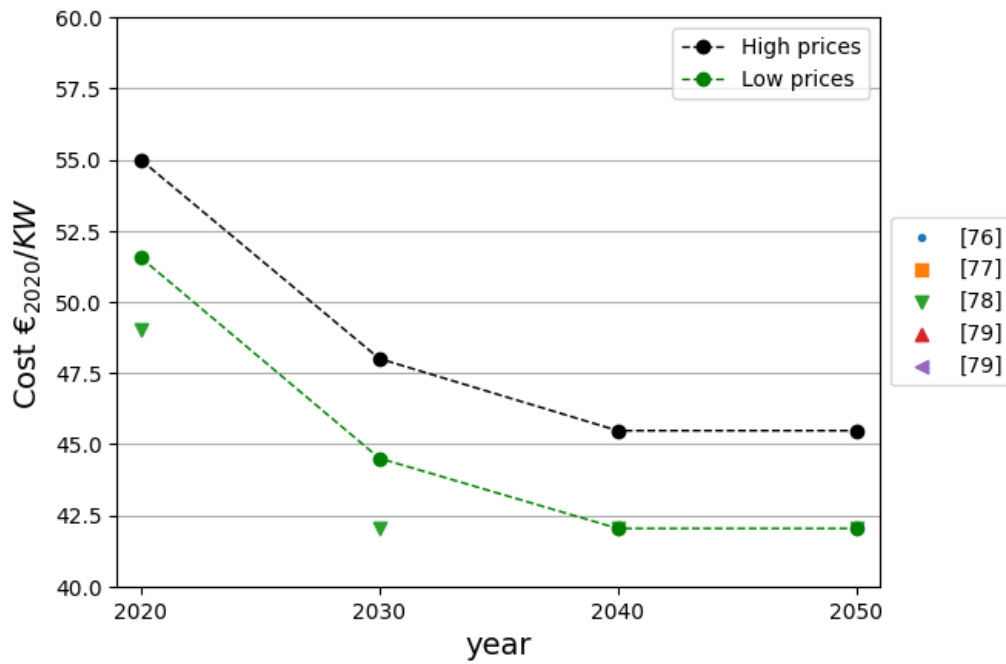


Figure 3.6: The cost of a hydrogen boiler plotted with time. To get the boiler unit price for this model the cost has to multiplied by 40. This plot was modified to illustrate the trend lines clearly, the unmodified data points plot can be seen in appendix A figure A.4. The points in the legend corresponds with the source in the bibliography[76–79].

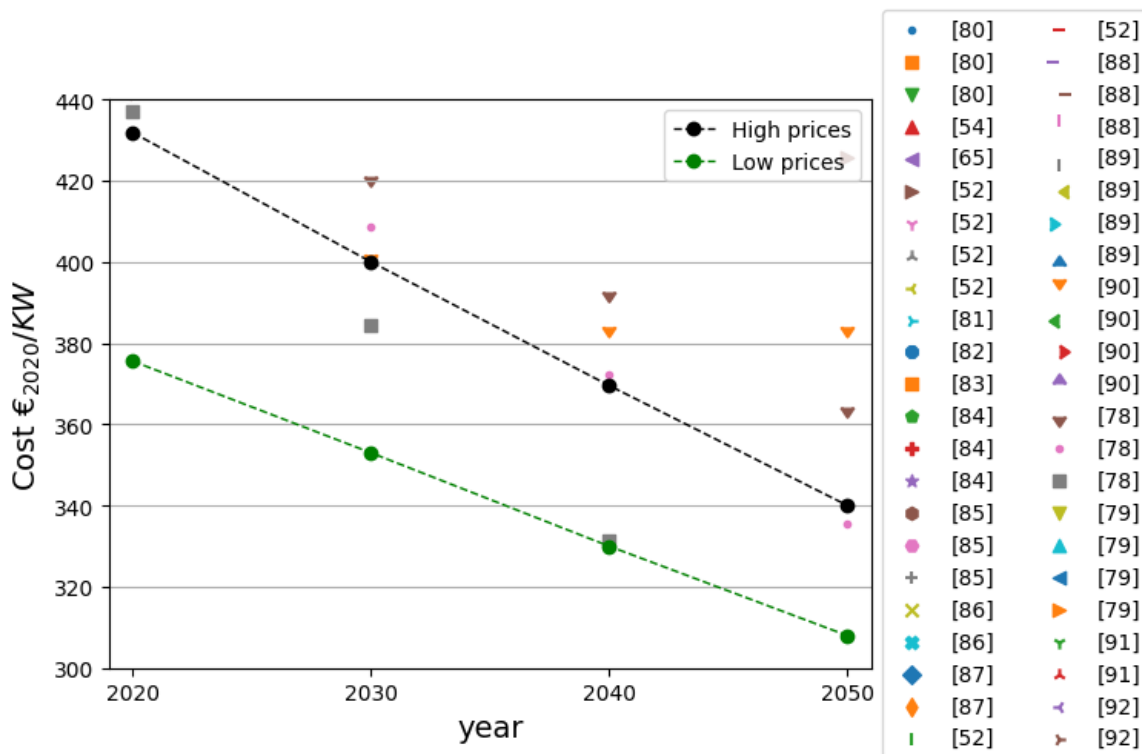


Figure 3.7: The heat pump system cost plotted with time. To get the heat pump unit price for this model the cost has to be multiplied by 7.9. This plot was modified to illustrate the trend lines clearly, the unmodified data points plot can be seen in appendix A figure ???. The points in the legend corresponds with the source in the bibliography[52, 54, 65, 78, 80–92].

3.3.7. Inverter

There are three inverters in this model; one for the solar panels, the batteries system and fuel cell. In the searching process for inverters cost projections, it was noticed that there are more projection about inverters related to a PV system. For that reason, the data set mostly consists of inverters for solar applications and it is assumed that other inverter types will follow the same trend. The trends are presented in figure 3.8, which includes the cost of the inverter unit.

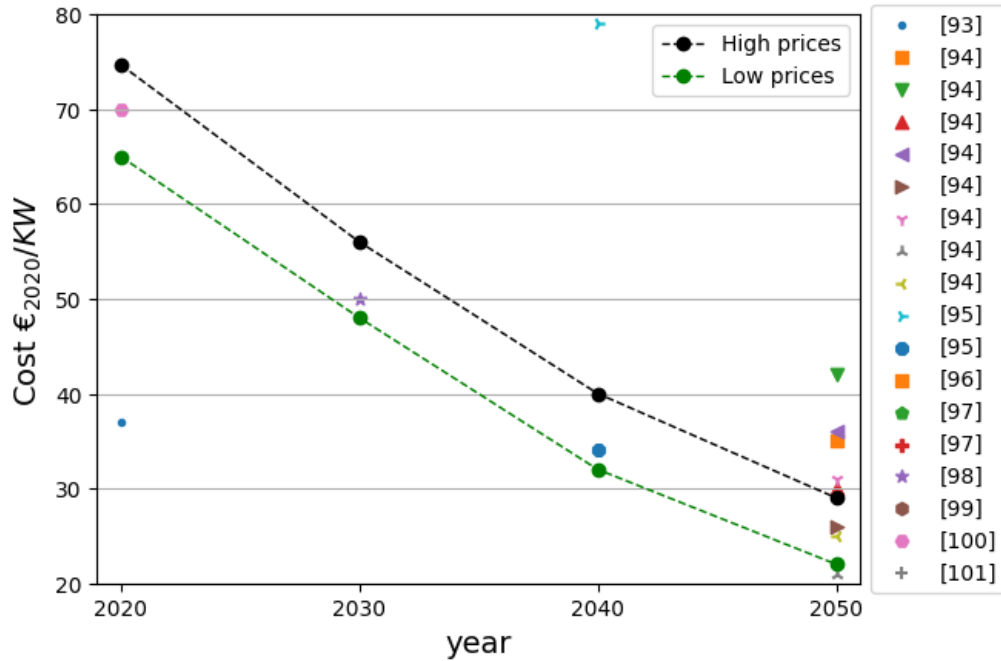


Figure 3.8: The inverter unit cost plotted with time. This plot was modified to illustrate the trend lines clearly, the unmodified data points plot can be seen in appendix A figure A.6. The points in the legend corresponds with the source in the bibliography[93–101].

4

System optimisation

This chapter will elaborate how the optimal system size is determined. First the optimisation algorithms will be introduced with the objective function and the optimisation variables. Then the scenarios that were used in the simulations will be discussed. At the end there is an overview of all the simulation scenarios and cases.

4.1. Optimisation algorithm

The optimal size of the hybrid system is estimated by using the GenOpt add on for TRNSYS, which is an optimisation program that searches for the minimum of a given cost function[102]. GenOpt has a library of pre-installed optimisation algorithms that are used for this research.

The optimisation program uses two algorithms to find the optimal solution. At first it will start searching with Particle Swarm Optimisation(PSO) algorithm for a set generation. After this the Hooke-Jeeves optimisation(HJO) algorithm will continue the search.

GenOpt can only change the variables which defines the size of the system, these are; the number of roof panels, the park multiplier, rated power of the electrolyser and fuel cell, the capacity of the batteries and the hydrogen tank size. These variables and their domain will be further elaborated on in subsection 4.1.2.

Particle Swarm Optimisation

Particle Swarm Optimisation is an algorithm which uses potential solutions to make a "swarm" to evaluate the optimal point. This is done by iterating various generations of a group of particles around the field of all possible solution or the search-space. Eventually all the particle points will move to the optimal point in the search-space[103][104].

Hooke-Jeeves Optimisation

Hooke-Jeeves Optimisation algorithm is a pattern search algorithm which moves the observed point set steps per iteration on the search-space. The next iteration in this process repeats from the previous optimal point[105][104].

4.1.1. Objective function

In this work the main goal of the objective function is to minimise the LCOE of the system. However, the focus is not exclusively on the LCOE of the system. The optimal solution is one in which the LCOE is the lowest while satisfying set conditions. These conditions include the SSR value being 1 [%] and the park multiplier being as small as possible. The conditions are met by adding penalty functions to the objective function that will be constraining the SSR value and the park multiplier. These will force the optimisation algorithm to search for an optimal solution while having the SSR and park multiplier as close to their desired value as possible. The constraints will further be discussed in the following paragraphs.

SSR penalty function

One of the main requirements of this system is not to be very reliant on the grid. This is achieved by having the self sufficiency ratio (SSR) of the system as small possible. There would be a trade off here, as a lower SSR

will mean that the system will need to be bigger to meet the peak demand. Therefore, the SSR constraint was set to be 1 [%]. This will mean that the system can supply the instantaneous load demand with power from the grid for 1 [%] of the total energy demand.

To integrate this constraint into the objective function a penalty was introduced for values that differ from the set SSR value of 1 [%]. This penalty function can be seen in equation 4.1. The constant in front of the penalty function is to amplify the punishment of the constraint. There is also a quadratic term which prevents this penalty function from becoming negative. An unwanted effect of the quadratic term is that if the SSR difference is smaller than 1, the value would be squared to get a very small number. This will then influence the constant and reduces the punishment of the penalty function. When the SSR values were filled in as decimals, the absolute value will be squared which makes it a very small number. This led to the optimisation algorithm estimating an optimum results that did not have the SSR value around 1 [%]. Therefore, a distinction between the strict and less strict objective function was created. The penalty function with the whole number will be the stricter one and be used first to reach the 1% SSR value faster. Hereafter, the less strict objective function will be used for the further optimisation process.

$$K_{SSR} = C(SSR - 1\%)^2 \quad (4.1)$$

- K_{SSR} , the penalty value on the objective function if the set SSR value is not met
- C , a weight constant added to the penalty function
- SSR , the self sufficiency ratio of the system [%]

Park multiplier penalty function

This model has the possibility to put a solar park next to the neighbourhood to increase energy generation for high energy demand cases. The solar park will be facing the south direction and will generate more energy per panel than the roof mounted solar panels. Hereby, the solar park can become the dominant source of energy for this model. This will contradict the decision to use roof mounted solar panels. Therefore, a constraint was introduced to penalize the objective function if the algorithm tries to maximize the solar park size. This is achieved by squaring the park multiplier term in this model, which is a value that defines the size of the solar park. In this model the solar park will be divided into steps with each step representing 189 solar panels or rated power of 64.26 [KW_p]. The park multiplier represents how many steps are used for the solar park in each simulation. The penalty function for the park multiplier can be seen in equation 4.2.

$$K_{\text{parkmultiplier}} = (\text{parkmultiplier})^2 \quad (4.2)$$

- $K_{\text{parkmultiplier}}$, the penalty value on the objective function for having a solar park
- park multiplier , the number of solar park steps that represents the solar park size

The whole objective function can be seen in equation 4.3, which include the penalty functions and LCOE. Having a longer objective function will increase the difficulty for the optimisation algorithm to reach an optimal solution. Therefore, the park multiplier penalty function is only used if it is clear that without the extra generation the SSR value can not reach around 1 [%]. Otherwise, the objective function will only consist of SSR penalty function and LCOE. For the cases ran in this research, for the fully electrical neighbourhood the combination of the base, EV & heat demand and for the integrated hydrogen neighbourhood the base & HV and base, HV & heat demand resulted to need a solar park next to the neighbourhood.

$$F = C(SSR - 1\%)^2 + LCOE + (\text{parkmultiplier})^2 \quad (4.3)$$

4.1.2. Optimisation variables

The optimisation algorithm can only change the sizing of the system. They can be seen in table 4.1. As most of these variables were also optimised in the previous work, the domain and step size were kept the same[18]. Changed or added variables will be further explained in the next paragraphs. For all the main components it was chosen to have the step size the same as its minimum allowed size. If the algorithm chooses the smallest allowed size, the system will still be a PV-battery-electrolyser-fuel cell system.

Table 4.1: The search-space and step sizes that are used for the optimisation algorithm.

Variable	Domain	Step size	Description
N_{nee}	0.5 - 20	0.5	Number of modules on the roof per orientation
N_{sww}	0.5 - 20	0.5	
N_{nnw}	0.5 - 20	0.5	
N_{sse}	0.5 - 20	0.5	
Parkmultiplier	0 - 40	1	Multiplication factor of the step defined solar park
$P_{ratedEly}$	120 - 15000 [KW]	120 [KW]	Rated power of the electrolyser
$P_{ratedFC}$	120 - 15000 [KW]	120 [KW]	Rated power of the fuel cell
$E_{ratedBatt}$	50 - 12000 [KWh]	50 [KWh]	Rated battery size
V_{tank}	50 - 1500 [m ³]	50 [m ³]	Hydrogen tank volume

Roof Solar modules

There are 6 orientations for the roofs of the houses, including the roofs oriented towards the south and north. The south orientation will have the maximum amount of solar panels possible on the roof and no solar panels will be placed on the roofs with a north orientation. The number of solar panels located on a roof with a specific orientation is indicated by N . From the previous work it was estimated that a maximum of 20 panels can be set on each roof[18]. As every orientation has an even amount of houses in the neighbourhood, the step size of 0.5 indicates that there will be an extra panel every other house.

Park multiplier

The park multiplier has a maximum of 40 steps, the same amount of steps as the solar roof variable. By keeping this the same the search-field of these variables can be comparable and the algorithm will search both of their search-space at the same pace.

4.2. Scenarios

In this section the scenarios that are researched will be introduced. There is a fully electrical scenario and an integrated hydrogen scenario. The fully electrical scenario has 4 different load profiles and the integrated hydrogen scenario has 3. The combination of scenario and load profiles will be addressed as cases of the model.

In table 4.2 all the scenario and their cases can be found. The cases will be further referenced by the abbreviation that are used in this table.

Table 4.2: The scenarios with their corresponding load profiles can be seen in this table. These will shape the cases that are researched. Their abbreviations are given in this table and will be further used in the paper to refer to them. The crossed out boxes were not researched because the base load profile does not change between the two scenarios.

Scenario	Years	Load profile			
		Base	Vehicle	Heat demand	Vehicle + heat demand
Fully electrical	2020	C-E _{Base}	C-E _V	C-E _H	C-E _{V+H}
	2030	C-E _{Base}	C-E _V	C-E _H	C-E _{V+H}
	2040	C-E _{Base}	C-E _V	C-E _H	C-E _{V+H}
	2050	C-E _{Base}	C-E _V	C-E _H	C-E _{V+H}
Integrated hydrogen	2020	C-E_{Base}	C-H _{2V}	C-H _{2H}	C-H _{2V+H}
	2030	C-E_{Base}	C-H _{2V}	C-H _{2H}	C-H _{2V+H}
	2040	C-E_{Base}	C-H _{2V}	C-H _{2H}	C-H _{2V+H}
	2050	C-E_{Base}	C-H _{2V}	C-H _{2H}	C-H _{2V+H}

4.2.1. The fully electrical scenario

The fully electrical scenario has electricity as the only energy source that can be consumed by the neighbourhood. In this scenario, the round trip effectiveness of storing energy in hydrogen gas can be better studied.

Base(C-E_{Base})

The household electrical load demand of the neighbourhood will be the only load input of the simulation. This load profile will resemble that of the Smart Load Management(SLM) load profile from previous work[18]. This case will be the base case of this research, every other case here after will add an extra demand on the load profile.

Electric vehicle(C-E_V)

EV are introduced to the neighborhood and their electrical demand. The electrical demand for charging the EV will be added to the base electrical demand to make the load demand of the neighbourhood. This will create the case of the base with EV.

Heat demand(C-E_H)

Here every house will have a heat pump installed and will provide the heating of the house. It is assumed that the heat pumps are electrical. The electrical demand of the heat pumps will be added to the base electrical demand. This will create the case of SLM with heat demand.

Vehicle & heat demand(C-E_{V+H})

EV will also be added to the heat demand case. This will then create the case which include the base, EV and heat demand.

4.2.2. The integrated hydrogen scenario

In this scenario the consumption of hydrogen gas will be added to the model. The system will need to be able to provide electricity and hydrogen gas to the neighborhood.

Hydrogen powered vehicle(C-H_{2V})

HV and their hydrogen consumption demand will be introduced to the neighbourhood. The base electrical demand will be accompanied by a hydrogen recharging demand from the HV. As Hydrogen gas will be stored in the tanks, the recharging mechanism will have access to this stored hydrogen. This will create the case of the base with HV.

Heat demand(C-H_{2H})

The houses will have a hydrogen heating component installed, which is a hydrogen boiler. The hydrogen boiler will meet the heat demanded of the house by burning hydrogen gas from the storage tanks. Also, the base electrical demand needs to be met. This will create the case of the base with heat demand for the integrated hydrogen scenario.

Vehicle & heat demand(C-H_{2V+H})

The two hydrogen consumption demand of the vehicle and heating will then be combined to make the load demand. The case will include the base, HV and hydrogen heating.

5

Result & discussion

A sensitivity analysis of several parts of the model was performed at the start of this research. The findings of the sensitivity analysis and the changes that were made to the model will be presented in this chapter.

Following the sensitivity analysis, the main findings will be discussed, to answer the research question: *What is the techno-economic feasibility of a grid-tied PV-battery-electrolyser-fuel cell power system for a household area in the Netherlands which is either fully electrical or hydrogen integrated?*

First the technical feasibility of the PV-battery-electrolyser-fuel cell-power system will be discussed. Followed by an economical and cost analysis of this system. At the end the reliance of hydrogen storage of the system will be discussed.

5.1. Sensitivity analysis on the model

The sensitivity of the model output to the SSR penalty function, simulation start time, battery charge cycle constrains and the elctrolyser mechanics were analysed.

5.1.1. SSR penalty function

As mentioned in section 4.1.1, the SSR value will need to be as close as possible to SET-SSR value of 1 [%]. With closer SSR values the simulation results will have a better comparison between each other. The changes of the LCOE are researched by changing the SSR penalty function. The two variables that are going to change are the SET-SSR and weight constant of the penalty function. The SER-SSR values were chosen to be 1, 3, 6 and 10 [%]. The chosen weight constant values were 60, 120, 210 and 300. For every SET-SSR value four optimisations are run with the four different weight constant values. From these optimisations, the results with the lowest LCOE for every SET-SSR value were chosen to represent the global optimum of the search-field. The LCOE and their corresponding SSR value for each iteration of this sensitivity analysis is reported in table 5.1.

Table 5.1: The LCOE and the corresponding SSR value results from the optimisation of the various SET-SSR and weight constant. The first number is the LCOE and the second italic number is the SSR value. The green boxes represent the lowest value for each SET-SSR value.

Weight constant	SET-SSR			
	1[%]	3[%]	6[%]	10[%]
C = 60	1.07 [€/KWh] <i>0.439 [%]</i>	1.09 [€/KWh] <i>0.837 [%]</i>	1.04 [€/KWh] <i>1.580 [%]</i>	1.33 [€/KWh] <i>2.276 [%]</i>
C = 120	1.10 [€/KWh] <i>0.364 [%]</i>	1.09 [€/KWh] <i>0.837 [%]</i>	1.28 [€/KWh] <i>1.453 [%]</i>	1.09 [€/KWh] <i>1.614 [%]</i>
C = 210	1.23 [€/KWh] <i>0.415 [%]</i>	1.17 [€/KWh] <i>0.856 [%]</i>	1.20 [€/KWh] <i>0.822 [%]</i>	1.17 [€/KWh] <i>1.845 [%]</i>
C = 300	4.81 [€/KWh] <i>0.730 [%]</i>	1.10 [€/KWh] <i>0.811 [%]</i>	1.11 [€/KWh] <i>0.822 [%]</i>	1.05 [€/KWh] <i>1.569 [%]</i>

As can be seen in table 5.1, the SET-SSR value of 6 [%] resulted in the lowest LCOE value of 1.04 [€/KWh]. The corresponding SSR value is 1.58 [%], which is higher than all the other highlighted values. The system for SET-SSR value of 6 [%] is allowed to extract more energy from the grid and the system size will be smaller relative to the other results. This was observed as the long-term storage capacity reduced with higher SSR value. The fuel cell, electrolyser and hydrogen tank capacities all reduced, which reduced the cost of these systems. A higher SET-SSR value will allow the system to extract more energy from the grid, which will reduce the system sizing and the LCOE.

An other observation is that the battery size did increase with an increase in SET-SSR value. This is the effect of having less fuel cell power at night. The batteries will need to provide more energy at night and the optimisation algorithm will therefore increase the battery size.

It was chosen to use the SET-SSR value at 1 [%] for further optimisations. The reason for this is that independence from the grid is a bigger priority than LCOE reduction from higher allowed SSR value.

In this analysis all the minimum LCOE are from a weight constant value of 60, with the SET-SSR value of 10 [%] being the exemption. Therefore, it was chosen to use the weight constant value of 60 for further optimisations.

5.1.2. Simulation start time

For the previous work the simulation started at the beginning of the calendar year and ran for a year. As the neighbourhood is located in the Netherlands, in the beginning of the year it will be winter, where there is lower generation. Previously the model's hydrogen tank would start with a certain level of charge to be used in the winter period. For that reason, a hydrogen sustainability penalty function was implemented in the previous work[18]. This hydrogen sustainability penalty function is applied to reduce the dependency on purchasing hydrogen as stated in subsection 3.2. This extra penalty function gives the optimisation algorithm an extra condition that has to be met in finding the optimal solution, which adds extra search time to the optimisation process.

For this research it was chosen to find a start time in which the system will not need to consume hydrogen gas at the beginning of the simulation. The start time was moved from hour 0 to 1464, which is the second of March. On the second of March the SOC of the hydrogen storage tank changed from reducing to increasing. This date was observed from the decentralised scenario with SLM case from the previous work[18]. Because of this change the hydrogen sustainability penalty function can be taken away. This led to a significant reduction in optimisation search time.

5.1.3. Constrains on the batteries charge cycle

For the previous work the model had a control mechanism for the batteries that allowed the batteries to only discharge after reaching a SOC of 85 [%]. The discharge constrain was set to control the batteries cycling to prolong the lifetime of batteries. A disadvantage is that the batteries can not be utilised in days that the discharge constrain is not met.

This control mechanism was removed and as a result the batteries can now provide power at any time above the lower SOC limit. Also, the lifetime of the batteries was kept the same at 15 years, as it was assumed that there is a charge controller strategy that will control the duty cycle of the batteries. The removal of the discharge constraint led to the batteries providing around 10 [%] more energy to the load, while not having any significant change on the LCOE. The system did become more self-sufficient as the system needed 35 [%] less energy from the grid compared to without this alteration. This led to a decrease of 1 [%] in SSR value.

5.1.4. Electrolyser cycle regulator

It was noticed that the electrolyser will cycle around 17125 times during the lifetime of the system. An electrolyser can cycle or be turned on/off for 5000 times before being significantly degraded and have to be replaced[106]. For the previous work it was assumed that the lifetime of the electrolyser was halved to compensate for the intermittent nature of the energy source. Halving the electrolyser lifetime increased the amount of times the electrolyser has to be replaced, which leads to a higher cost. For this research it was chosen to not use this assumption and find a method to reduce the electrolyser cycle. Achieving this will mean that the electrolyser lifetime does not need to be halved and will lower the replacement count.

The electrolyser will turn on or remain on if the surplus power send to the electrolyser meet the minimum power threshold, which is a fraction of the rated power of the electrolyser. For the previous work the minimum power was set at 10 [%] of the rated power of the electrolyser. This was changed to 10 [%] of the smallest step

size of the electrolyser power, which is 120 [KW]. This was done to reduce the possibility that the surplus power would be around the minimum power threshold over a day.

At the start and end of the day, when surplus power is around this threshold, the most on/off cycles occur. Therefore, reducing the periods when surplus power is around this threshold was investigated by changing the operational period of the electrolyser. The electrolyser will only be operational in a season where there is substantial over generation and from 11 to 18 o'clock. The period chosen was in the summer from the 9th of May (3096 [hr]) to the 4th of July (4440 [hr]). To keep the electrolyser operational in the specified time frame, the electrolyser was allowed to take power from the batteries if the PV generation can not meet the electrolyser power needs. This significantly reduced the cycle of the electrolyser to 1425 over the system lifetime and the electrolyser lifetime was changed back to 60000 from 30000 hours.

The result of this was that the surplus energy in the rest of the year will not be stored as hydrogen gas and be sold to the grid. This led to a significant energy transfer to the grid, which caused a steep increase in the revenue inflow. The revenue recouped 56% of the cost of the system. This did decrease the LCOE value from 0.98 to 0.27 [€/KWh], but here the LCOE is highly inflated on the possibility of selling this excess energy. Therefore, it was chosen to not implement these changes for the rest of the research.

Forecasting method

A forecasting method was also looked into to reduce the cycling of the electrolyser. As the weather data and the load demand is known, time steps where there is surplus power can be identified beforehand. This was done for a forecast of 1,2- and 3-time steps ahead of the present time step. In each of these time step the model will evaluate if there is enough surplus power to operate the electrolyser. The electrolyser would only turn on if there is enough surplus power in the forecasted time steps. This does not apply when the electrolyser is already turned on, as it will stay operational till there is not enough surplus power. For example, if in the present time step it is estimated that there is enough surplus power to switch on the electrolyser and for all the next 3-time steps there is enough surplus power to function the electrolyser, the electrolyser would turn on.

The forecasting method reduced the electrolyser cycles by around 60 [%], the electrolyser cycles can be seen in table 5.2. The LCOE had no significant change as the sizing of the system did not change in this analysis. Only the SSR value increased, but it stayed under the SET-SSR value of 1 [%]. This is an effect of the electrolyser having less time to produce and store hydrogen. There will be less stored energy, which has to be compensated by the grid. The reduced operational time of the electrolyser also had an effect on the amount of energy sold to the grid. As the operational time was less, there were more time steps that the electrolyser will not use the surplus power. This led to an increase of energy sold to the grid and a ten times greater revenue stream of the system.

Table 5.2: The change in cycling of the electrolyser with the time step forecasting method. The corresponding LCOE and SSR value are the result of the optimisation with the forecast time steps.

Forecast time	SSR [%]	LCOE [€/KWh]	Electrolyser cycles
Base case	0.026	0.9806	17125
1 time step	0.857	0.9666	6600
2 time step	0.845	0.9656	6275
3 time step	0.871	0.9660	6825

At the end of this analysis, it was noticeable that the simulation run time has significantly increased with the forecasting. The optimisation already takes 2 to 7 days to find an optimal solution before the forecasting was added. Hereby, it was chosen to leave the forecasting out of the model for the rest of the research.

With a method to reduce the cycling of the electrolyser feasible with fair results, changing the electrolyser characteristics back for the further research is not needed. Therefore, the electrolyser lifetime has stayed at 60000 hr and the reduction of the minimum power for the electrolyser is kept. These changes will keep the electrolyser cycles and replacements lower than that of the previous work. Which will eventually lead to a lower electrolyser cost that is more comparable to the simulation with the forecasting method.

5.2. An analysis of the cases

In this section the main results of the optimisation algorithm will be analysed for the various cases. The optimised sizing variables of the cases can be seen in appendix B, for both the fully electrical and integrated hydrogen scenarios. These are followed by some parameters that resulted from the simulation.

The trends that were observed from the technical and economic analysis will be elaborated on followed by the reliance of the system on stored hydrogen. Each subsection will consist of the results and a small discussion.

In chapter 3 the low and high projected prices were estimated for the PV, batteries, electrolyser, fuel cell, hydrogen heating boiler, heat pumps and inverters components. These price projections were used in the model. For now, only the low projected prices were used as input for optimisation of the model. The same sizing results were then used to run the model with the low and high projected prices of the components. The results which are presented here are from the low projected prices. In subsection 5.2.4 the cost difference between the low and high projected prices results will be addressed.

5.2.1. Technical feasibility analysis

In this subsection the technical feasibility for the cases will be presented. Primarily the simulation of the cases will be evaluated if they are sufficiently self-reliant from the grid or from an external energy source. A case is deemed technically feasible if the SSR value $\leq 1.4\%$. Table 5.3 presents which cases are technical feasible and which is not within the power generation boundary conditions considered in this study as described in subsection 4.1.2.

Table 5.3: In this table the cases which are technical feasible and not feasible are presented. The cases which are presented in green are technical feasible, the cases which are presented in red are not feasible. A discussion on why they are feasible or not will be in presented in subsection 5.2.1. The cases with an asterisk have a PV park attached to their system.

Scenario	Years	Load profile			
		Base	Vehicle	Heat demand	Vehicle + heat demand
Fully electrical	2020	C-E _{Base}	C-E _V	C-E _H	C-E _{V+H} *
	2030	C-E _{Base}	C-E _V	C-E _H	C-E _{V+H} *
	2040	C-E _{Base}	C-E _V	C-E _H	C-E _{V+H} *
	2050	C-E _{Base}	C-E _V	C-E _H	C-E _{V+H} *
Integrated hydrogen	2020		C-H _{2V} *	C-H _{2H}	C-H _{2V+H} *
	2030		C-H _{2V} *	C-H _{2H}	C-H _{2V+H} *
	2040		C-H _{2V} *	C-H _{2H}	C-H _{2V+H} *
	2050		C-H _{2V} *	C-H _{2H}	C-H _{2V+H} *

This subsection will first discuss the fully electrical scenario followed by the integrated hydrogen scenario. At the end of the subsection a small comparison between both scenarios will be presented.

Fully electrical scenario

The SSR values for the fully electrical scenario can be seen in figure 5.1. The case of C-E_{V+H} for the year 2020 did not have a SSR value smaller or equal than 1.4 [%]. All the other cases did result in a SSR value smaller or equal than 1.4 [%].

The lowest value obtained for 2020 C-E_{V+H} case was 2.1 [%] SSR value. A short sensitivity analysis of the SSR to the weight constant used in the objective function, during optimisation, did not result in lower SSR values. Having a 2.1 [%] SSR value makes the 2020 C-E_{V+H} case technical not feasible for this research.

Additionally for the 2020 C-E_{V+H} case, the hydrogen tank will be depleted for a month in the winter period. In the simulation this will be the 12th month (last month), which is February. With the depleted hydrogen tank, the fuel cell cannot provide enough power to meet the demand and the system had to extract the deficit energy from the grid.

For all the other cases the tank did not deplete and there was no indication of any technical issues present.

A short discussion

The simulations demonstrated that the system would extract more energy from the grid in the winter period for every case, when on average demand exceeds the generation over the day.

The 2020 C-E_{V+H} has the highest load demand of all the cases because the electrical vehicle and heat pumps demands are included. Hereby, when optimising the 2020 C-E_{V+H} case, the PV system and tank size reached

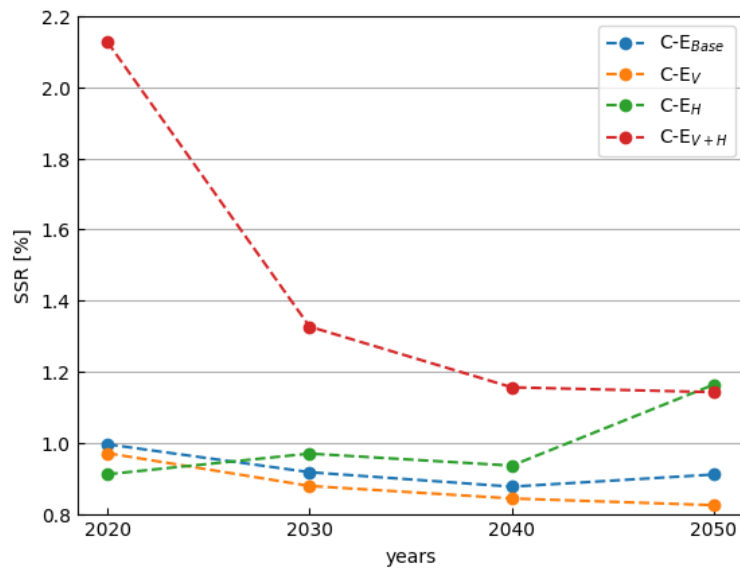


Figure 5.1: The SSR results are illustrated for the fully electrical scenario with a SSR weight constant of 60. The years represent the results of the model if the system was constructed in set year.

the maximum allowed number of the domain for their optimisation variables.

To lower the 2020 C-E_{V+H} case SSR value, more energy must be generated in combination with a bigger long-term storage capacity. This can be achieved by increasing the PV power or for this case increase the PV park size. Increasing the PV park size is done by increasing the park multiplier value.

These changes must be combined with increasing the long-term storage capacity. In this model this is done by increasing the tank size. This will lead to a higher amount of hydrogen gas being stored that will prevent the tanks to be depleted in the winter period. With these changes a SSR value of around 1 [%] can be achievable.

Integrated hydrogen scenario

The integrated hydrogen scenario is a system where both electricity and hydrogen gas are being consumed by the neighbourhood. Therefore, a self-sufficiency ratios(SSR) can be estimated for both energy sources which can be seen in figure 5.2.

For the C-H_{2H} case, there are big differences between the SSR values of the electricity and the hydrogen energy sources. The hydrogen SSR_{H₂} value stays above 25 [%] over the years, more than a quarter of the hydrogen gas consumption will be provided by an external source. The need to get hydrogen gas from an external source is also noticeable in the SOC of the hydrogen storage tank as can be seen in figure 5.3. The SOC of the tank depleted a month and half before the end of the simulation, then the hydrogen flow rate demanded by the boilers will need to be provided from an external source. The depleted tank also curtails the hydrogen storage function, as when the SOC reduces to 0 [%] the hydrogen volume flow rate to the fuel cell also reduces to 0. The fuel cell cannot function anymore to provide extra power to the system.

At the beginning of the plot in figure 5.3 there a period during which the tank becomes fully depleted. This is because of the extra hydrogen consumption added by the hydrogen boilers, which made the chosen start time of the simulation not optimal for the C-H_{2H} case.

With HV added to the neighbourhood for the C-H_{2V} case, the hydrogen demand of HV are too big for the system. In figure 5.2 it is noticeable that the hydrogen SSR_{H₂} value stays around 96 [%], which means that most of the demanded hydrogen gas will be delivered by an external source. This was also noticeable in figure 5.4 where the SOC of the tank would be depleted on the first day and there after will not increase for the rest of the simulation. During the entire simulation, on a daily basis, the hydrogen gas consumption by HV exceeds the hydrogen gas generation of the electrolyser. The depleted tank let the fuel cell to only be operational on the first day of the simulation. This meant that for the C-H_{2V} case there are no hydrogen storage function and that the fuel cell will be idle for the rest of the simulation year. In figure 5.2 the electrical SSR_E values for the case C-H_{2V} are relatively high because the results for this case was not fully optimised to find the lowest SSR values.

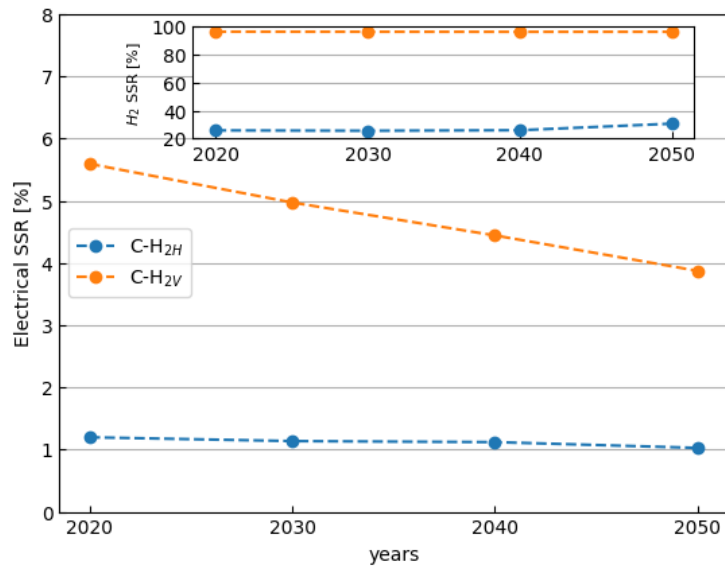


Figure 5.2: The SSR results are illustrated for the attained results of integrated hydrogen scenario. The years represent the results of the model if the system was constructed in set year. The big plot presents the electrical SSR_E values, which is the percentage of electrical energy that the system takes from the grid. The small plot represents the hydrogen SSR_{H_2} values, which is the percentage of hydrogen gas demand that was taken from an external source. The optimisation for the case C- H_{2V} were stopped after the PSO section, as mid optimisation it was noticed that the system has no hydrogen storage function. The results for C- H_{2V+H} was not searched for, as the case C- H_{2V} already had no hydrogen storage function.

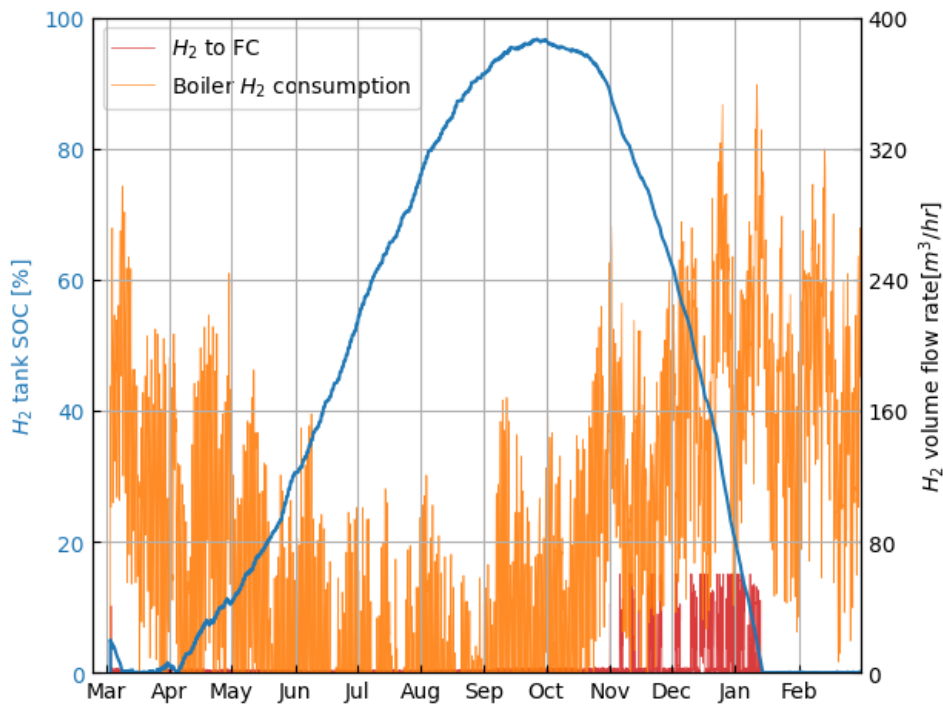


Figure 5.3: On the left axis the SOC of the hydrogen storage tank can be estimated over the simulation time of one year, the SOC is represented by the blue line. On the right axis the volume flow rate can be estimated for the fuel cell and hydrogen boiler. These are dependent on the electrical demand and heat demand of the neighbourhood. The plot presents the data of C- H_{2H} case of year 2020.

Because the model could not be used to estimate feasible results for the integrated hydrogen scenario with HV, it was chosen to not run the model for the combined case of hydrogen heating and HV. Both case of C- H_{2V} and C- H_{2V+H} are considered not feasible for the model. As these cases have no hydrogen storage function, they will be exempt from the rest of the results discussion.

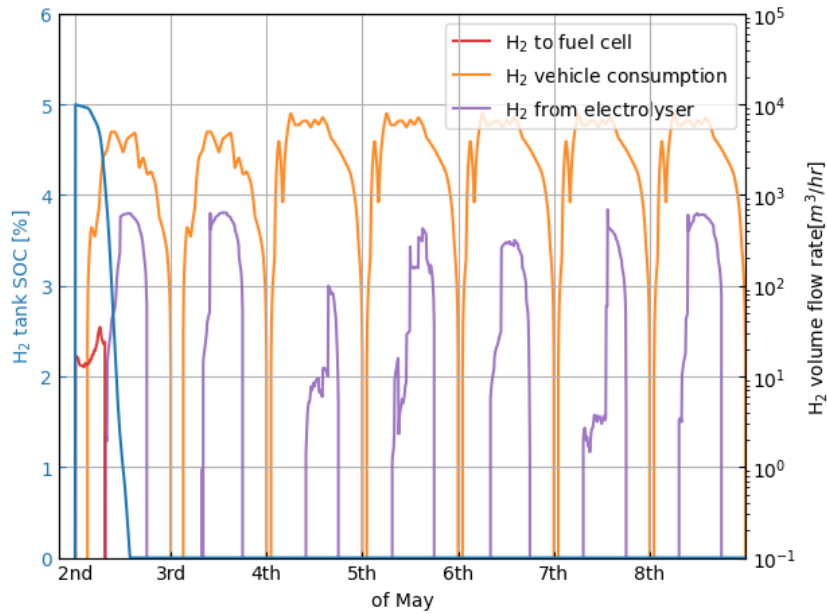


Figure 5.4: On the left axis the SOC of the hydrogen storage tank can be estimated for the first week of the simulation, the SOC is represented by the blue line. On the right axis the volume flow rate can be estimated for the fuel cell, HV and electrolyser. The flow rate of the fuel cell is dependent on the electrical demand and the amount of stored hydrogen gas. The flow rate of the HV is dependent on an average private vehicle usage. The flow rate of the electrolyser is dependent on surplus power. The plot presents the data of C-H_{2V} of year 2050.

A short discussion

A reason for the big differences between the electrical and hydrogen SSR values in figure 5.2 is that the optimisation algorithm SSR penalty function was only implemented for the SSR_E value of electricity energy source. There was no other limitation applied on the SSR_{H₂} value of hydrogen energy source. Therefore, the optimisation algorithm only takes the extra cost of buying external hydrogen gas into the estimates. This meant that the optimisation algorithm did ignore the dynamics of hydrogen gas flow added into the system, which lets the system be very reliant on an external hydrogen source. As a requirement for the system is to be sufficiently self-reliant from an external source, the hydrogen SSR_{H₂} values of more than 25 [%] which is higher the requirement of ≤ 1.4 [%], makes the case C-H_{2H} technical unfeasible. This is only because of the hydrogen demand side of the system, the system is sufficiently self-reliant for the electrical energy demanded by the neighbourhood.

The depleted tank period at the start of the simulation shows that the start time chosen was not optimal for the C-H_{2H} case. Starting the simulation around the beginning of April can achieve a better start time as previously discussed in subsection 5.1.2. The optimal start time looks to be related to the consumption and generation of hydrogen gas; therefore, the optimal start time will be different for the cases in the integrated hydrogen scenario.

To include the HV demand in the model a bigger production of hydrogen gas is needed or accept buying the hydrogen gas demanded by the HV from an external source.

Comparing fully electrical to integrated hydrogen

Unfortunately, all the integrated hydrogen scenario cases were not technical feasible with the model as of now. For the fully electrical scenario only the case with the highest demand was technical not feasible. For both scenario the model had issues when the load demand got very high. This means that the domain size of the optimisation variables will need to be further analysed and expended if possible. This can be done by adding a solar park to all the cases and having the upper domain of the solar park rated power as big as the area around the neighbourhood allows. Doing this does take away the decentralised essence of the solar system, which was the chosen scenario to research from Atkins work[18].

The model will also need to consider the dynamics of both electrical and hydrogen energy sources. This was achieved for electrical energy by restricting the dependency of taking electrical energy from the grid, the model will then need to adjust its sizing of the various components to meet the demand. This process will

have to be implemented for hydrogen energy in the system. By achieving this the hydrogen storage tank will not get depleted for a long period of time and the functionality of storing hydrogen will be present.

5.2.2. Economical and cost analysis

This subsection will elaborate on the economic and cost parameters of the system for the cases. As previously done, first the fully electrical scenario results will be discussed followed by the integrated hydrogen scenario. At the end of the subsection a small comparison between both scenarios will be presented.

Fully electrical scenario

In figure 5.5 the LCOE result can be seen for each case. For each case the LCOE reduced with the years and the smallest LCOE is 0.21 [€/KWh] for C-E_{Base} case in year 2050. The 2050 C-E_{Base} has the smallest energy consumption as in the year 2050 the annual electrical consumption will be reduced by 20 [%]. This combined with the system cost reduction led to LCOE of 2050 C-E_{Base} case being the lowest.

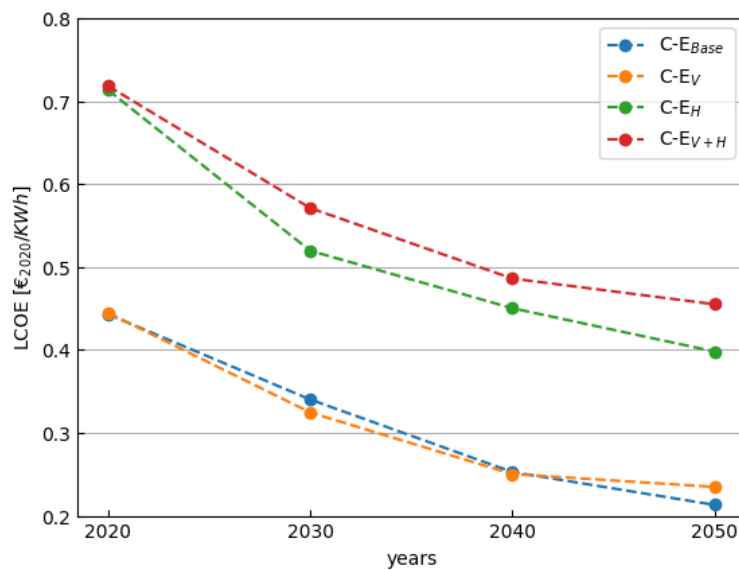


Figure 5.5: The LCOE results are illustrated for the fully electrical scenario. The years represent the results of the model if the system was constructed in set year.

When comparing the LCOE of this model to those of the previous work, only the 2020 year can be compared, as the previous work had no simulation for the rest of the years. It can be noticed that the LCOE of the cases C-E_{Base}, C-E_V and C-E_H reduced by 48, 47 and 45 [%] respectively. For the cases where EV and head demand was added, the previous work did not apply the SLM load profile for the houses in the neighbourhood. This caused the system of the previous work to be bigger in size when compared to this research for these two cases. The C-E_{Base} uses a similar load profile as the previous work and therefore it can be concluded that the changes made in the sensitivity analysis had a significant improvement on the LCOE.

Compared to the other LCOE values found from the literature study, especially that of the grid-tied hybrid system, it is noticeable that this model resulted in a significantly bigger LCOE values.

In figure 5.6 the change in PV system size and cost can be seen. The PV system cost reduced over the years, even if the system size increased. A reduction in component cost can be seen for all the component prices that were researched in chapter 3.

It was noticed that the component sizes for PV, electrolyser and fuel cell increased much more for C-E_{Base} case than the rest of the cases. This can be seen in figure 5.6 where the PV system size increased significantly with the years for the C-E_{Base} case. The reason for this is that the optimisation algorithm determined optimal system size to meet the load demands and thereafter kept reducing the LCOE by increasing the PV system size. By increasing the PV system size more than needed, there will be more over generated power. The over generated power will be sold to the grid. With more over generated power the revenue stream from selling electricity increased. With a higher revenue stream the net total cost of system will be lower, which reduces the LCOE of the system. For the 2020 C-E_{Base} case it resulted that after the demand was met, the pv system

can generate an average revenue of 2.45 [€/W_p] from selling energy to the grid over the whole lifetime of the system. Even with the highest PV prices of 1.008 [€/W_p] in 2020, the PV system can generate a substantial profit. The C-E_{Base} case had a revenue around 1.8 M€ or 8 [%] of the total cost of the system for 2020, which grew to 3.7 M€ or 28 [%] of the total cost for 2050. Therefore, the increase in PV size led to more energy being generated and more excess energy being sold.

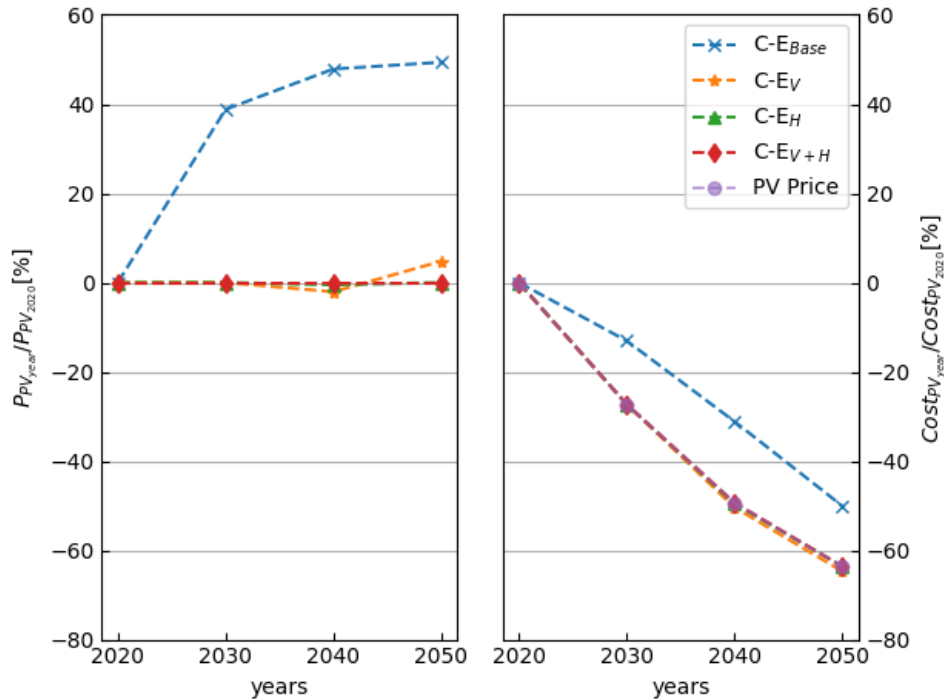


Figure 5.6: The left plot presents the size difference of the PV system for every case of the fully electrical scenario. The differences are estimated to year 2020. The right plot presents the price of the PV system and cost difference. The legends data correspond to both plots.

A relationship was noticed between the load demand profile and the system size, especially for the C-E_V case. In figure 5.7 the profile of the 2020 C-E_V case can be seen for one week in the summer and winter seasons. From the load profile curve, it is noticeable that most of the EV demand are in the evening hours where the PV production has stopped. To keep the system sufficiently self-reliant, the hybrid system were sized to meet the demand during the months with the least generation because of low irradiance. A consequence of this is that the roof PV system has a lot of over generation during the summer season, which made a significant revenue stream. Here the optimisation found an optimal system size in which demand is met by strongly increasing PV, rather than increasing the long-term storage systems size. The optimisation algorithm resulted to be more eager of increasing the PV size because of its cheaper cost compared to the storage systems. The 2040 C-E_V case had the highest revenue at 2.6 M€ or 14 [%] of total cost. The rest of the years have around the same revenue stream value. For this case solar park was not used, as the extra solar power was not needed. The cases which included heat demand had no significant revenue stream and the roof PV system size reached maximum capacity. The C-E_{V+H} case did have a solar park attached to it, but the solar park was not maximized for every scenario.

In figure 5.8 the cost of the various component for the system size of C-E_{Base} case can be seen. For the C-E_{Base} and C-E_V cases, the PV system is the most expensive component followed by the hydrogen storage tank and the fuel cell. For the cases of C-E_H and C-E_{V+H} the hydrogen storage tank is the most expensive component followed by the PV system and fuel cell.

The result of the PV component being one the most expensive component is related to its size. The PV price per unit is the lowest of the main components, but for all the cases the PV system size is the biggest. Therefore, the PV system has one of the biggest absolute costs.

The fuel cell high cost is related to the multiple unit replacement it has, on average being replaced 12 time

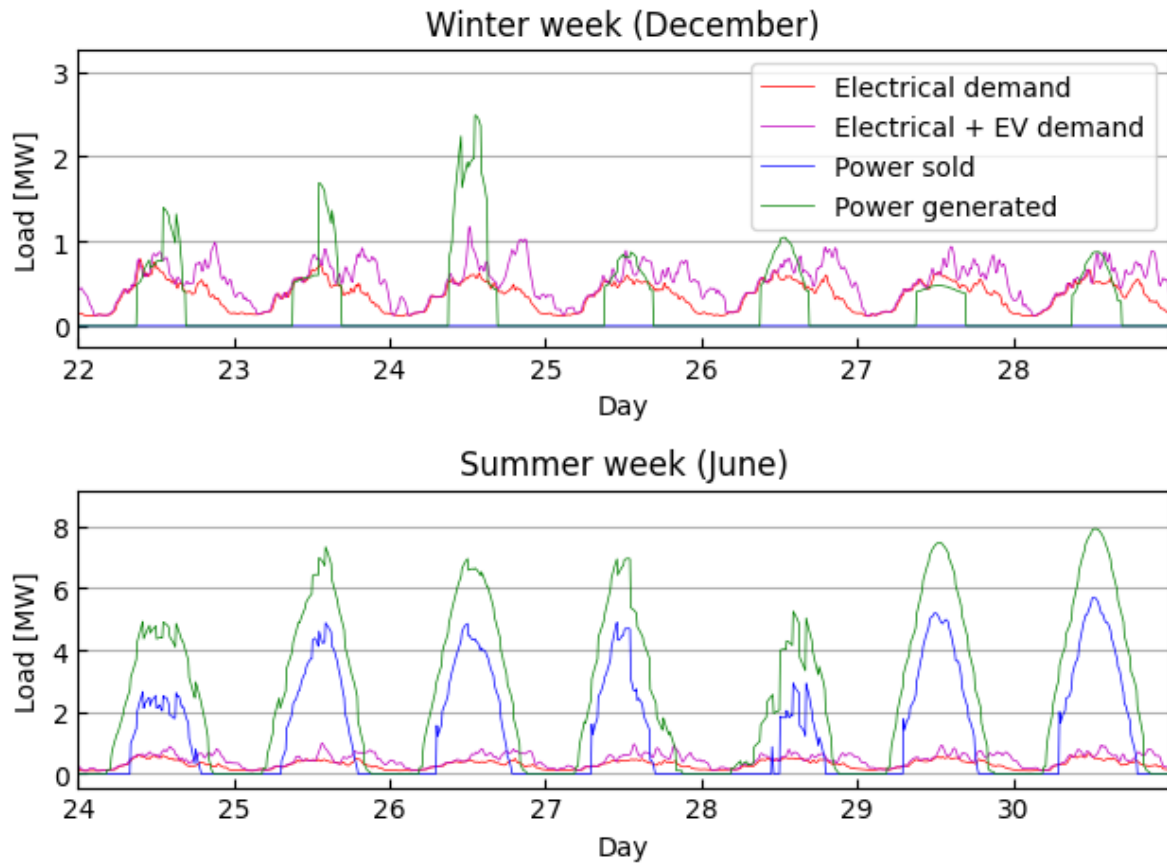


Figure 5.7: The demand and generation of electricity are presented here for a summer and winter week. The data are taken from the results of the 2020 C-EV case. The legend data correspond to both plots.

over the lifetime of the system.

Eventually the hydrogen storage tank becomes the most expensive component for all the cases.

For all the cases the PV system and the fuel cell cost reduced the most over the years, which contributed the most to the reduction of the total system cost. The big reduction in the PV system cost is because of its size, the large PV system size in combination with the reduction in the PV system price resulted in the large cost reduction.

The reduction of fuel cell price had a big influence in the fuel cell component cost reduction. Even in the cases where the fuel cell size did not change over the years, the fuel cell component cost was still one of the biggest reduced.

A short discussion

The reduction of LCOE over the years is strongly influenced by the price decrease of the components which were discussed in chapter 3. This influence is also present for the PV cost, as the PV cost reduction followed the price reduction over the years.

It was noticed that the LCOE from this research was significantly bigger than that of the grid-tied hybrid system from the literature study. As the systems of those studies were mostly in high irradiance locations, they will have a more robust hybrid system that can generate and store more energy if needed. Also those systems were not restricted to have a high degree of self-reliance. As those systems had around a fifth of the load being met by the grid, this had caused their system to be smaller in size compared to if they had the same self-reliance restriction applied in this research.

For the cases that included heat demand, the heat demand is so large that it causes the roof PV system size to reach maximum capacity, which takes away the option of increasing the PV rated power. This prevented the optimisation algorithm to increase the revenue stream to reduce the LCOE. The PV park penalty function prevented the C-EV+H cases to maximise the PV park size, as the penalty to increase the PV park size is bigger

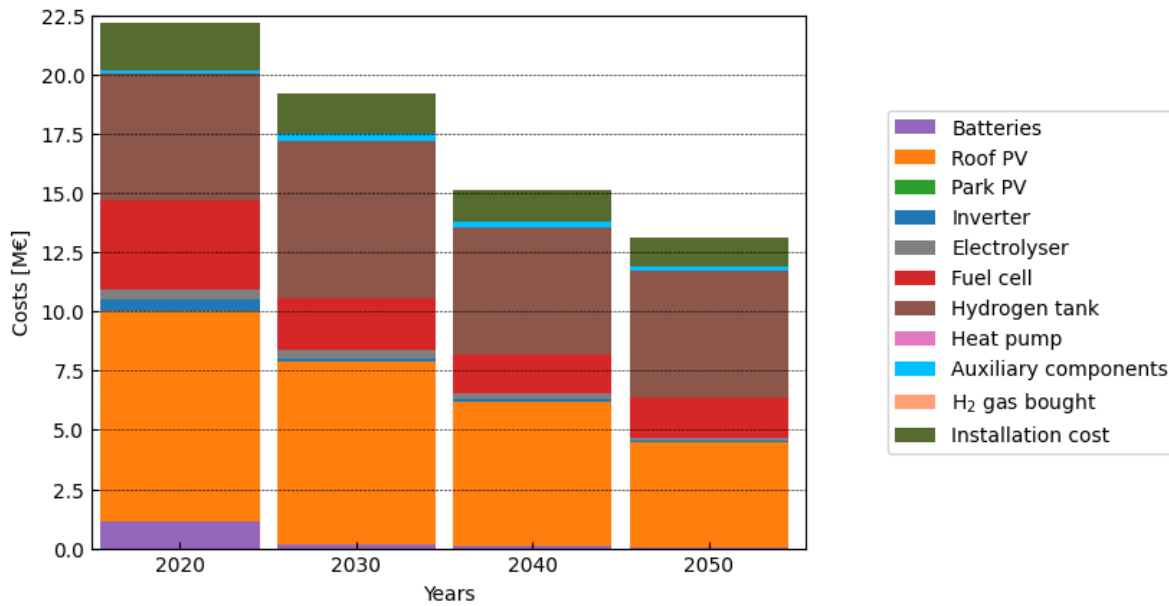


Figure 5.8: The total cost breakdown can be seen with its corresponding components. Every component of the hybrid system can be seen in the legend, while some components are not present in the chart for this case. This chart represents the component cost of the C-E_{Base} case.

then the benefits of reducing the LCOE.

Every case eventually has the tank as the biggest expense. This is because the tank size does not change significantly over the years and the tank price does not change. This led to the cost having little to no change over the years, while the other main components did reduce in cost.

Integrated hydrogen scenario

The LCOE for C-H_{2H} case can be seen in figure 5.9. There is a reduction in LCOE as was noticed for the fully electrical scenario. Here also the reduction in component prices combined with reduction in electrical load demand led to the reduction of LCOE.

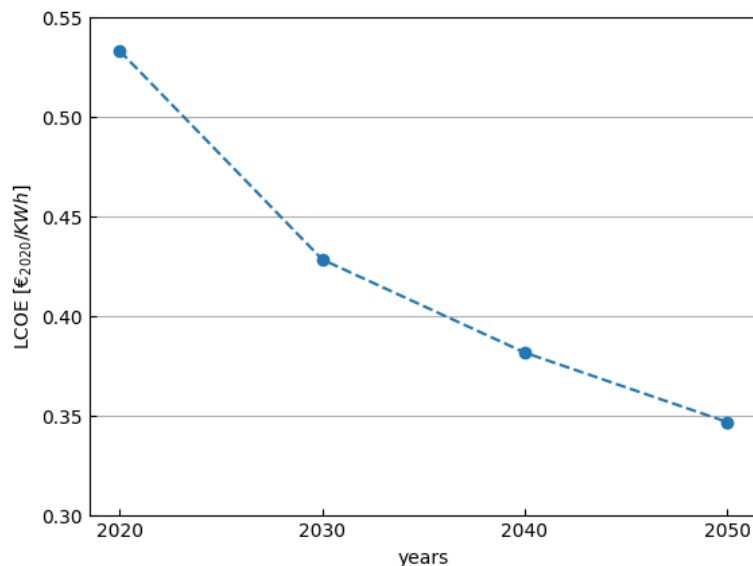


Figure 5.9: The LCOE results are illustrated for the C-H_{2H} case. The years represent the results of the model if the system was constructed in set year.

In figure 5.10 the total system cost breakdown of C-H₂H case can be seen.

For the C-H₂H the tank cost is the biggest expense for the system, followed by the PV system and then the hydrogen gas bought from an external source. The effects of the high hydrogen SSR_{H₂} value can be seen in the system cost for C-H₂H as the cost of buying hydrogen is substantial high.

For the C-H₂H case the PV system cost is also the component which reduced the most over the years. The whole hydrogen storage system (electrolyser, fuel cell and tank) cost reduction also contributed significantly to the system cost reduction.

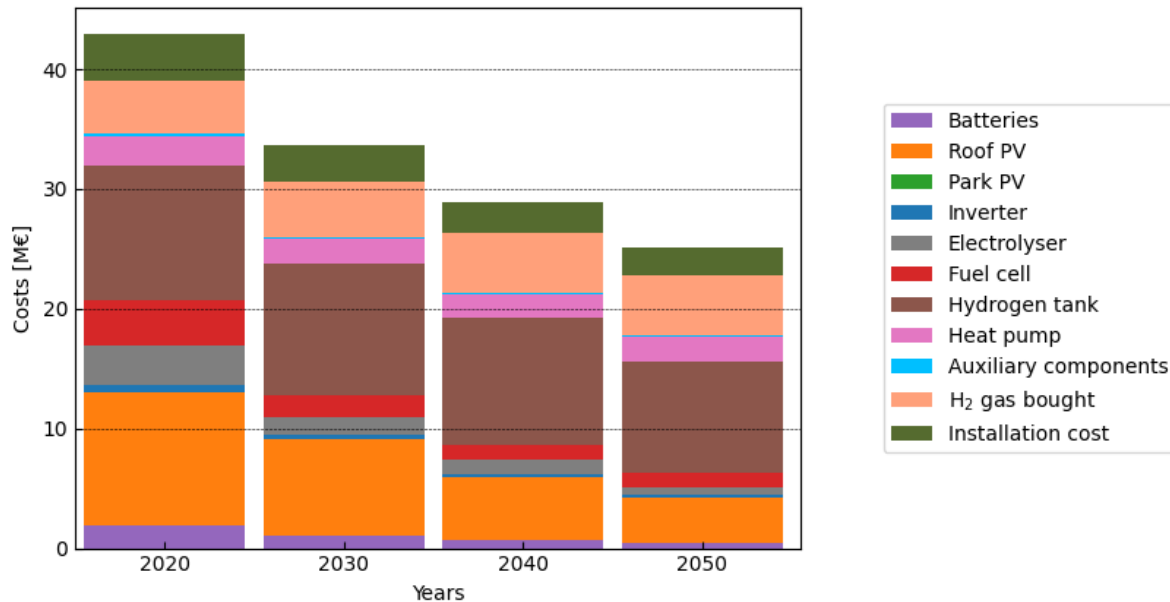


Figure 5.10: The total cost breakdown is illustrated for the C-H₂H case. Every component of the hybrid system can be seen in the legend, while some components are not present in the chart for this case.

A short discussion

As the hydrogen SSR value was not forced to 1 [%], the system was allowed to buy a significant amount of deficit hydrogen gas from an external source. The cost of buying hydrogen gas became the third biggest expense and also increased with the years. The optimisation resulted in a scenario where it was cheaper to buy hydrogen gas than to generate it, considering the cost of the pv, electrolyser and tank components.

Comparing fully electrical to integrated hydrogen

When comparing the two scenarios LCOE values, C-H₂H values were smaller than that of C-E_H case. This is because the system for C-H₂H case can buy the deficit hydrogen gas, which is cheaper than expending the hydrogen storage system. The two cases total system cost breakdowns can be seen in figure 5.11.

The smaller fuel cell and tank costs of the C-H₂H case is because of its smaller electrical demand compared to the C-E_H case. The C-H₂H system does not need to provide electrical energy to the heating component. The fuel cell system size and tank size is much comparable to that of the C-E_{Base}.

The tank cost has the biggest difference between these two scenarios, with the C-H₂H case tank cost being on average 36 [%] smaller than C-E_H case. A smaller tank is sufficient because the C-H₂H system can buy the deficit hydrogen gas from an external source at any time and the system did not need to provide electrical energy to the heating components.

The fuel cell cost for C-H₂H case is significantly smaller than C-E_H case, this is because of the electrical load demand being smaller and demanding less power from the fuel cell.

When analysing the results from the integrated hydrogen scenario cases, the loss of energy from converting electrical energy to hydrogen has to be taken into account. The electrolyser has an efficiency value which indicates how much hydrogen energy it produces from the electrical energy consumed. The efficiency values found for the electrolyser were on average 56 [%] (fully electrical scenario) and 53 [%] (integrated hydrogen scenario). The fuel cell also has an efficiency value, which is related to how much electrical energy it can produce from the hydrogen energy consumed. The fuel cell efficiency values were on average 54 [%] (fully

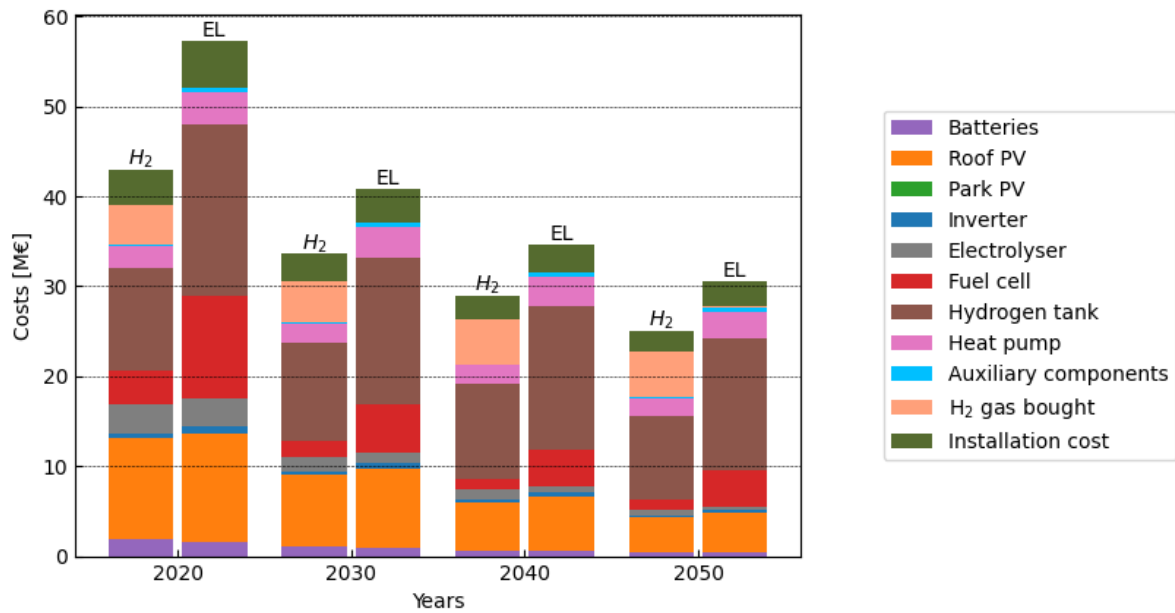


Figure 5.11: The total cost breakdown is illustrated for both scenarios for the base case with heating. The integrated hydrogen scenario is presented by the bar plot with H₂ on top of it and the fully electrical scenario is presented by EL. Every component of the hybrid system can be seen in the legend, while some components are not present in the chart for this case.

electrical scenario) and 59 [%] (integrated hydrogen scenario). When comparing the two scenarios cases that has heat demand included, the heat demand will be met by two different energy source. For the C-H₂H case the electrolyser has to be bigger to compensate for the loss of producing hydrogen gas. This was noticed as the electrolyser size for the C-H₂H case was on average 1.4 times bigger then C-E_H case and 5.3 times bigger then C-E_{Base}. The led to the elctrolyser being more expensive for the integrated hydrogen scenario.

By comparing the electrolyser efficiencies found in these simulations to the efficiency of 78 [%] achieved for other alkaline electrolyser system, the electrolyser system in these simulations had to bigger then what could have been expected[107]. The fuel cell efficiencies did not vary much to other PEM fuel cell system, other PEM fuel cell system can reach an efficiency of 60 [%][108].

5.2.3. The reliance on hydrogen storage

The reliance on hydrogen storage of the cases will be elaborated here. An estimation of which component provides the most electrical energy to the neighbourhood will be presented, which will give an indication to which storage system is used the most. As previously done, first the fully electrical scenario results will be discussed followed by the integrated hydrogen scenario.

Fully electrical scenario

An estimation was made of which fraction of load demand each component provides. The fractions of C-E_{Base} case can be seen in figure 5.12. For every case the PV system was the dominant component which provides the neighbourhood with the most energy. The grid will only contribute about 1 [%] of the load demand, which is forced by the SSR constraint.

What is left is provided by the storage systems. For the C-E_{Base} case it is noticeable that the system relies in 2020 more on battery storage and for the rest of the years relies more on the hydrogen storage system. This can be seen with the system sizing of the C-E_{Base} case, as the battery size decreased around five times after 2020 and while the electrolyser with the fuel cell increased in size. Therefore, the C-E_{Base} case became reliant upon the hydrogen storage system after the year 2020.

The rest of the cases has the battery as the primary storage system, which also provides the second biggest fraction of energy to the neighbourhood.

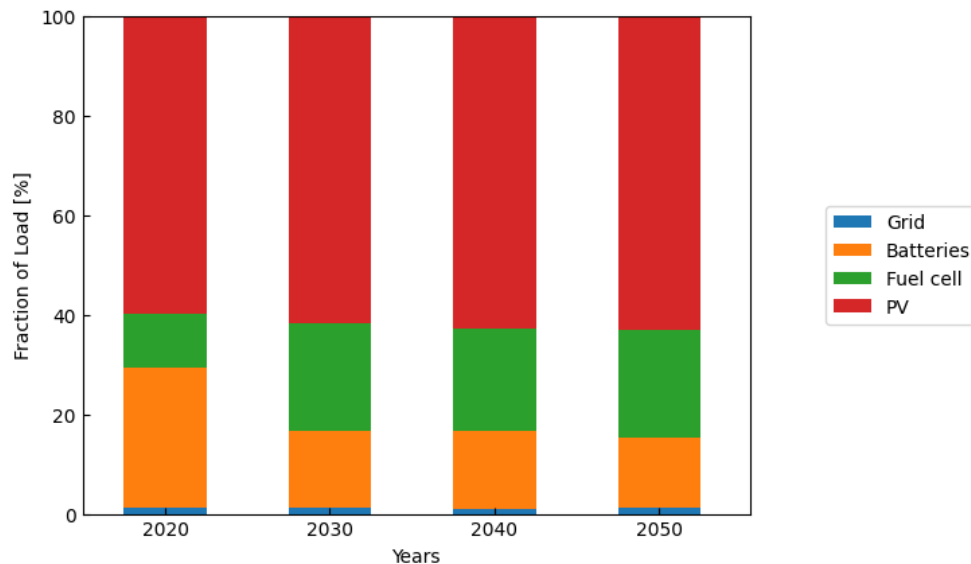


Figure 5.12: The stacked bar plot represents the fraction of the load demand that is provided by the given component. This fraction is estimated for the whole simulation period of one year. This plot presents the results from the C-E_{Base} case.

A short discussion

The differences in the fraction of load for the C-E_{Base} case can also be an effect of the optimisation algorithm approach taken. As previously stated in subsection 5.2.2, it is assumed that eventually the optimisation algorithm will try to reduce the LCOE by increasing the PV system size and selling more energy to the grid. This led to the hydrogen storage system size having the possibility to increase to a point that this system is big enough to become the primary storage system.

Having the battery system as the primary storage system is more straightforward when looking at the round efficiencies of both storage systems. A battery storage system has a round efficiency of ~95 [%] while a hydrogen storage system has a round efficiency of ~35 [%][6][109]. Therefore, a battery system would provide the same amount of energy with a smaller size and a lower system cost.

Integrated hydrogen scenario

The C-H_{2H} case component fractions can be seen in figure 5.13. They are also compared to the C-E_H case to illustrate the differences or comparisons between the two scenarios.

It is noticeable for C-H_{2H} that fuel cell provides a small fraction of the load demand and is four times smaller than that of C-E_H. For C-H_{2H} case the PV system is also the dominant energy source for the neighbourhood with the battery system as the primary storage system.

A short discussion

The small fuel cell fraction for the C-H_{2H} case is a result of the smaller electrical demand and the tanks depletion. As the system will need to store less electrical energy as hydrogen, the fuel cell provided energy will be less. The tank being depleted in the winter period also curtails the function of the fuel cell. This then curtails the amount of energy that the fuel cell can provide to the system. As the hydrogen storage system is less effective, the system must rely more on the battery storage system.

5.2.4. The cost differences between the low and high projected prices

In this subsection the results of the cost differences between the low and high projected prices will be presented. This will be done by addressing the total system cost between the two results and the total system cost breakdown.

The high projected prices had the biggest system costs for every case. This can be seen for C-E_{V+H} case in figure 5.14. The differences in the total system cost were on average around 23 M€ for the C-E_{V+H} case, which is the biggest difference between the cases. The total cost of the high projected prices was on average 35 [%] higher than for the low projected prices for all the cases.

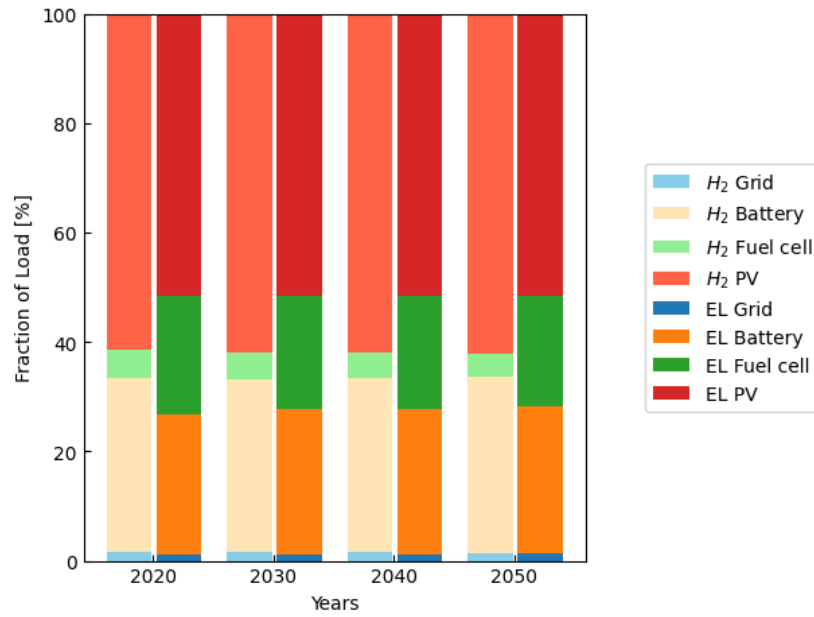


Figure 5.13: The stacked bar plot represents the fraction of the load demand that is provided by the given component. The bar plot with the lighter colours represents the fractions of C-H₂H case and the bar plot with the darker colours represents C-E_H. This fraction is estimated for the whole simulation period of one year.

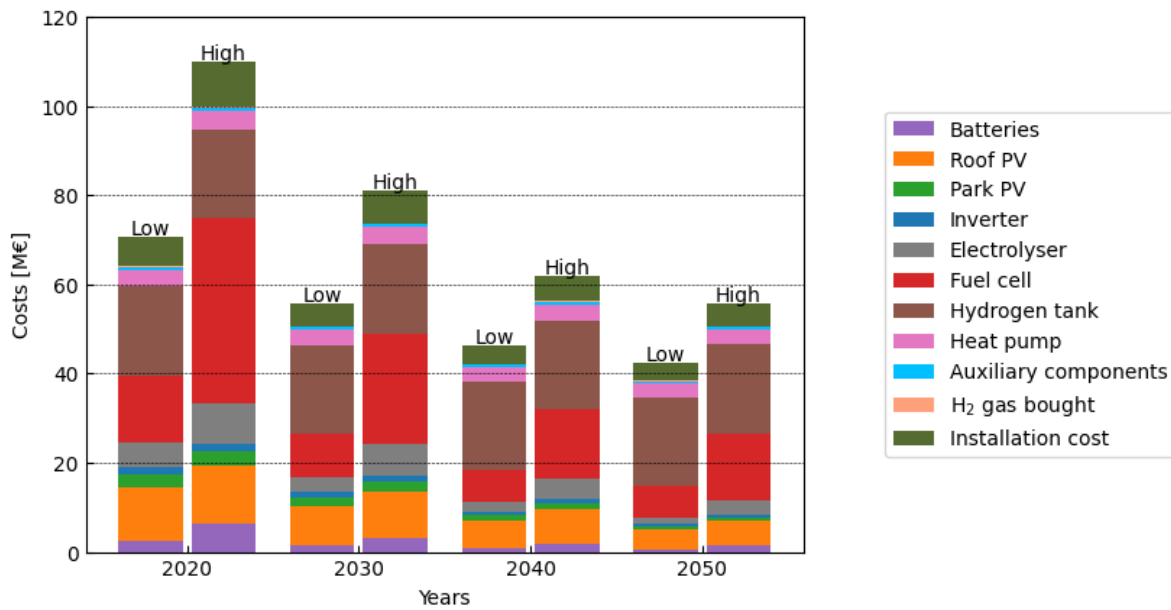


Figure 5.14: The total cost breakdown of C-EV+H case is presented for both low and high projected prices. The results for the low projected price are indicated by the bar plots with Low and the results for the high projected price are indicated by High. Every component of the hybrid system can be seen in the legend.

From the components the fuel cell cost was the biggest differences between the results from the low and high projected prices, with the biggest differences being for the year 2020. The fuel cell is also the component with the biggest cost for the results of the high projected prices. The reduction in fuel cell cost over the years was also the biggest compared to all the components, with biggest cost reduction occurring between 2020 and 2030.

A short discussion

As the C-E_{V+H} case has the biggest system size of all the case, increasing the components prices to the high projected prices led the cost being the biggest. Therefore, the difference in system cost between the low and high projected prices was the biggest for the C-E_{V+H} case.

6

Conclusion & recommendations

The conclusion and recommendation for future work will be discussed in this chapter. First, the main points and arguments which led to the conclusion of the research question: "What is the techno-economic feasibility of a grid-tied PV-battery-electrolyser-fuel cell-power system for a household area which is either fully electrical or hydrogen integrated?" will be listed.

Afterwards, a short discussion will be presented of the contribution of this work for the field. The chapter will end with a section of recommendations for future work, which will discuss the limitation of the model and relevant improvement points.

6.1. Conclusion

This thesis presented a grid-tied PV-battery-electrolyser-fuel cell power system model for TRNSYS program. This model can simulate a neighbourhood which is fully electrical or has integrated hydrogen. The model simulated a neighbourhood in Pijnacker Netherlands of which the system would be build in years of 2020, 2030, 2040 and 2050.

The trends over the years of the electricity and hydrogen gas demands were estimated, from which only the electricity demand reduced over the years. The price trends for these commodities were also estimated for the simulation years. To estimate the economic development of the system over the years, a projection of the main components prices were made. The PV, batteries, electrolyser, fuel cell, hydrogen heating component, heat pump and inverter prices were estimated for 2020, 2030, 2040, 2050.

The optimal system size is determined by the GenOpt optimisation program. This program uses PSO algorithm and Hooke-Jeeves algorithm to determine the optimal size variables to minimize the LCOE and keep the SSR value around 1 [%]. The cases that have been optimised can be seen in table 6.1.

Table 6.1: The scenarios with their corresponding load profiles can be seen in this table. Their abbreviations are given in this table.

Scenario	Years	Load profile			
		Base	Vehicle	Heat demand	Vehicle + heat demand
Fully electrical	2020	C-E _{Base}	C-E _V	C-E _H	C-E _{V+H}
	2030	C-E _{Base}	C-E _V	C-E _H	C-E _{V+H}
	2040	C-E _{Base}	C-E _V	C-E _H	C-E _{V+H}
	2050	C-E _{Base}	C-E _V	C-E _H	C-E _{V+H}
Integrated hydrogen	2020	C-E_{Base}	C-H _{2V}	C-H _{2H}	C-H _{2V+H}
	2030	C-E_{Base}	C-H _{2V}	C-H _{2H}	C-H _{2V+H}
	2040	C-E_{Base}	C-H _{2V}	C-H _{2H}	C-H _{2V+H}
	2050	C-E_{Base}	C-H _{2V}	C-H _{2H}	C-H _{2V+H}

Before the cases were optimised the model was analysed to find some improvement points. The simulation start time was moved from the 1st of January to the 2nd of March in order to avoid the hydrogen storage tank being depleted at the start of the simulation. The discharge constraints on the batteries were lifted, which led to an increase of battery energy provided. It was also proven that a forecasting method can effectively

reduce the electrolyser cycles, which will extend the lifetime of the electrolyser. These improvement points led to the model generating a lower LCOE compared to that of the previous work while still meeting the same requirements.

The results of the cases presented in table 6.1 estimated that all the cases which included additional hydrogen loads were not technical feasible for the roof mounted PV hybrid system modelled. The demand of hydrogen gas from the HV are to big compared to the hydrogen gas quantity that the model can provide. For cases C-H_{2V} & C-H_{2V+H}, this resulted in a fully depleted hydrogen storage tank for the duration of the simulation. The C-H_{2H} case only had a depletion period of the storage tank at the end of the simulation period. This made the system very reliant on buying external hydrogen gas in this period. But the SSR value of hydrogen energy source for this cases was not sufficiently self-reliant ($SSR_{H_2} \leq 1.4$ [%]).

For the fully electrical scenario only the case 2020 C-E_{V+H} was not technical feasible, because the system cannot be sufficiently self-reliant ($SSR_E \leq 1.4$ [%]). All the other cases are technical feasible.

From the economic and cost analysis of the cases it resulted that the LCOE of all the cases reduced with the years. The C-E_{Base} case LCOE reduced from 0.44 [€/KWh] in 2020 to 0.21 [€/KWh] in 2050, which was the lowest value of all the cases. The C-E_{Base} case also had the smallest load demand and total system cost. There is a strong correlation between the system cost and the price reduction from the projected components price. As the prices reduced over the years, the total system cost also reduced which reduced the LCOE. It was noticed that the optimisation algorithm after finding the optimal system size was eager on reducing the LCOE more by increasing the generated revenue from selling electricity to the grid which reduced the net system cost. This made the system quite reliant on the possibility and price of selling the over generated energy to the grid, which contradicts the self-reliance that is searched for system. It was also noticed that the optimisation algorithm was more prone to increase the PV size to meet seasonal demand peaks instead of increasing the long term storage systems. As PV system was cheaper to increase then the hydrogen storage system.

The LCOE was reduced compared to the previous work of Atkins, with the biggest contributor being the lower estimated cost of components[18]. But comparing the LCOE of this research to that from other works, it is noticeable that PV hybrid system in warmer climate over performed this proposed system.

It was noticeable from all the cost breakdown of the cases that the PV system and storage tank are the components which have the biggest costs. The integrated hydrogen scenario cases will need to buy a significant amount of hydrogen gas from an external energy source, the cost of buying hydrogen gas was a significant portion of the total system cost.

From the components that are capable of directly delivering power to the load, the PV system was the biggest contributor. The second biggest contributed component changed only for the C-E_{Base} cases. When the PV size increased significantly, the fuel cell became the second biggest contributor of power to the neighbourhood. The rest of the cases has the batteries as second biggest contributor of power to the neighbourhood. The fuel cell contributed a very low fraction to the neighbourhood electrical demand for the integrated hydrogen scenario. The added demand of hydrogen gas curtailed the function of the hydrogen storage system for this scenario.

A comparison between the fully electrical to the integrated hydrogen scenario led to these differences.

- For this model all the cases that have integrated hydrogen demand are not technical feasible by the requirements set of being sufficiently self-reliant (SSR_E & $SSR_{H_2} \leq 1.4$ [%]). For the fully electrical cases most of them are technical feasible.
- The PV system, fuel cell and storage tank sizes of C-H_{2H} case were all smaller than that of the C-E_H case. This led to a smaller LCOE for the integrated hydrogen scenario. This is because of the lower electrical demand of the C-H_{2H} case, which only consisted of the house electrical load. In comparison, the electrical demand of C-E_H case consisted of the house and heating electrical loads.
- The electrolyser system size was bigger for the integrated hydrogen scenario compared to the fully electrical scenario. Because of its efficiency the electrolyser will waste some of the electrical energy in the production of hydrogen gas. To meet the same heat demand, the electrolyser will need to consume more electrical energy to make sufficient hydrogen gas.
- For the integrated hydrogen cases, the hydrogen storage system was curtailed over all the simulations. In all the cases the hydrogen storage tank got depleted which obstructed the function of the fuel cell.
- The cost of buying hydrogen gas from an external source was significantly larger for the integrated

hydrogen scenario, which was caused by the depletion of the storage tank. The model resulted in a optimal point where it was cheaper to buy hydrogen gas then to increase production of hydrogen gas.

These points made it clear that a comparison between these two scenarios by this model is conflicted. As both scenario had different requirements for their self-sufficiency of their respected energy demands, a conclusion on which scenario is more beneficial will be inadequate.

Contribution to the field

This work presents a new version of the PV-battery-electrolyser-fuel cell power system developed by the PVMD group, which can simulate a fully electrical neighbourhood as well as a hydrogen integrated neighbourhood[16]. A projection can be seen of the technical feasibility and cost of this hybrid system over the years 2020 to 2050. The developed model also laid groundwork for a feasible hybrid system for an integrated hydrogen neighbourhood.

6.2. Recommendations for future work

As this model strived to simulate some feasible cases for both scenarios, there were some shortfalls. Here are some improvement points that can be made to the model:

- A bigger domain size for the optimisation variables. This can be done by either estimating a practical limitation on the size of the system on the spaces available or just applying the biggest system size developed as of now as the upper bound. By applying this some not technical feasible cases (especially 2020 C-E_{V+H}) can be better researched on what can make them technical feasible.
- A SSR constraint on hydrogen energy must be applied to the optimisation algorithm. This will keep the system more self-reliant for hydrogen gas and will lower the cost of buying hydrogen from an external source. For this model the same SSR penalty function for electrical energy must be applied for the hydrogen energy. This will increase the system size for the integrated hydrogen scenario and can lead to a better comparison to the fully electrical scenario.
- Applying a mechanism to find the optimal result with the minimum revenue stream of the system. This can be achieved by applying a penalty function for the increasing revenue stream. This will then force the optimisation algorithm to stop searching at the smallest system size that will meet the demand of the neighbourhood. This can also promote an increase of the storage systems size in the model. As these system are relatively more expensive then PV, it can increase the system cost and LCOE.
- A method to reduce the replacement number of the fuel cell. In this model the fuel cell is one of the most expensive components and is the main component that is replaced the most. Replacing the whole system leads to higher costs and doing this frequently over the lifetime of the system increase the cost significantly. Therefore, a method to increase the lifetime of the fuel cell will benefit the system cost and can help reduce the LCOE of the system.
- Estimating the cost projections of the hydrogen storage tanks. For this research the price of the storage tanks was kept constant over the years, which led to it being one the most expensive component of the system. It was assumed that storing hydrogen gas in a compressed cylindrical tank will not have any significant development, so the prices will not change. But as this system becomes more popular or a different hydrogen storage method becomes more economical, the price can change over the research period.
- Running the simulation for a region that has higher irradiance then the Netherlands. There was a big difference in the LCOE of the this work and that of other work, with systems in regions with higher irradiance having a low LCOE value. Running this model in a location with higher irradiance can reduce the LCOE value obtained and simulate other dynamic behaviours.
- Expanding the hybrid system to include other energy sources as wind power, biomass power plant or region specific energy sources (hydro power, tidal power, etc.). The extra energy source will cause changes in the generation behaviour of the model and will lead to different sizing of the PV, batteries, electrolyser, fuel cell components.

A

Components price trend curves

Here the price trend graphs with all the plotted points can be seen, which were presented in chapter 3.

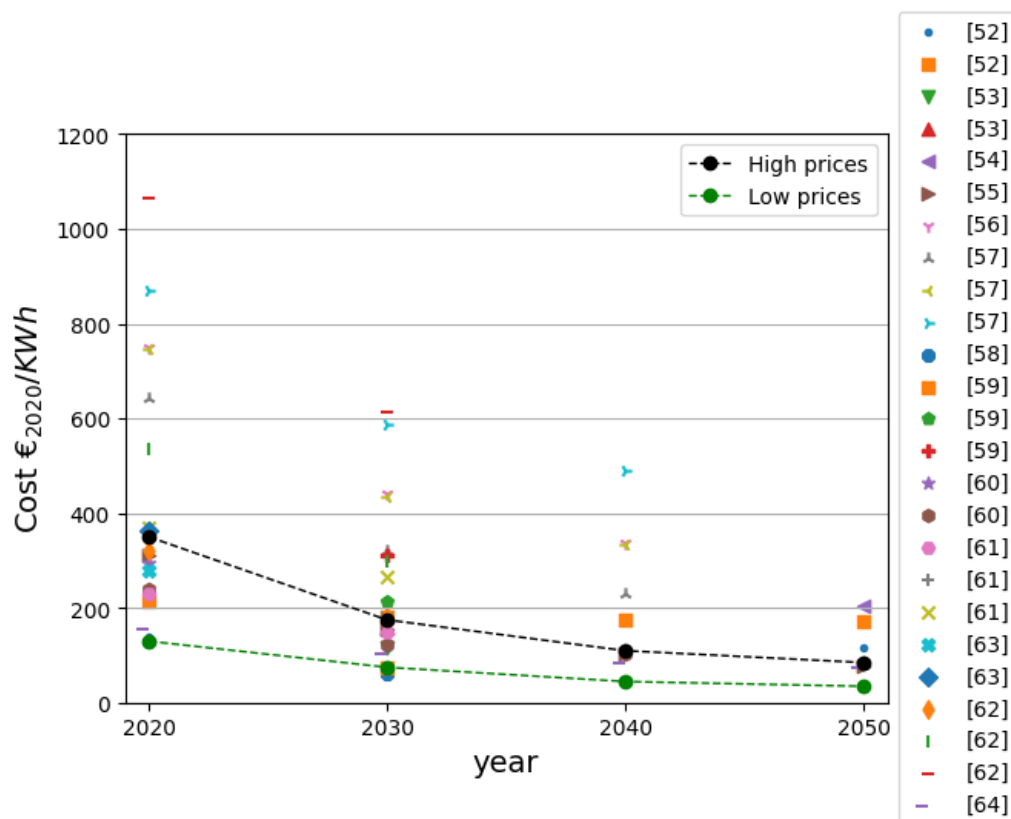


Figure A.1: The lithium-ion batteries system cost is plotted with time. The points in the legend corresponds with the source in the bibliography[52, 53, 55–61, 63, 64].

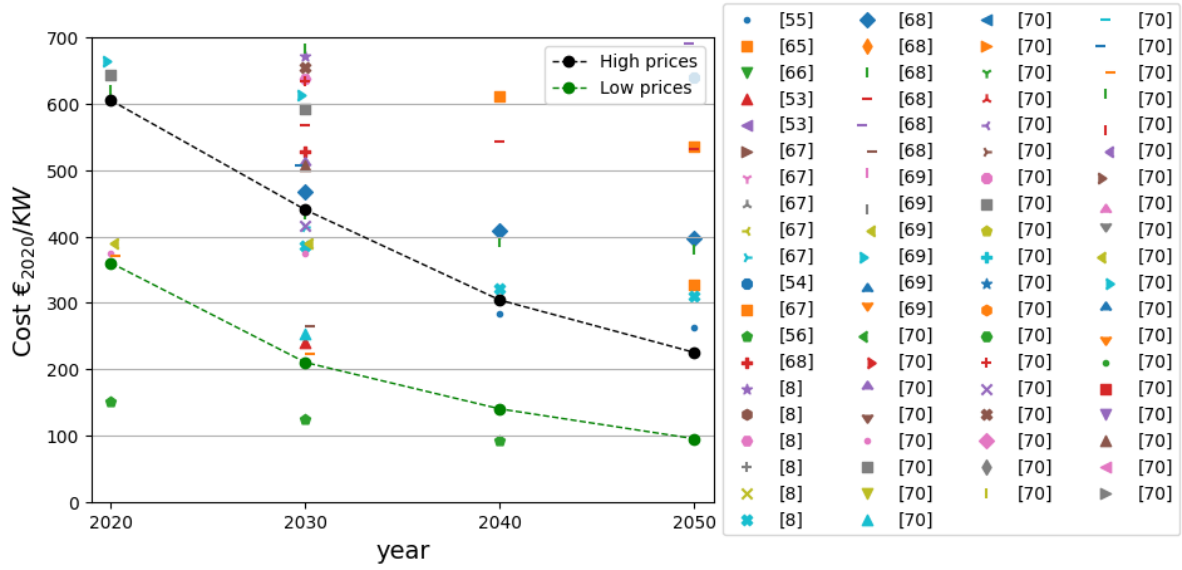


Figure A.2: The Electrolyser cost is plotted with time. The points in the legend corresponds with the source in the bibliography[8, 53–56, 65–70].

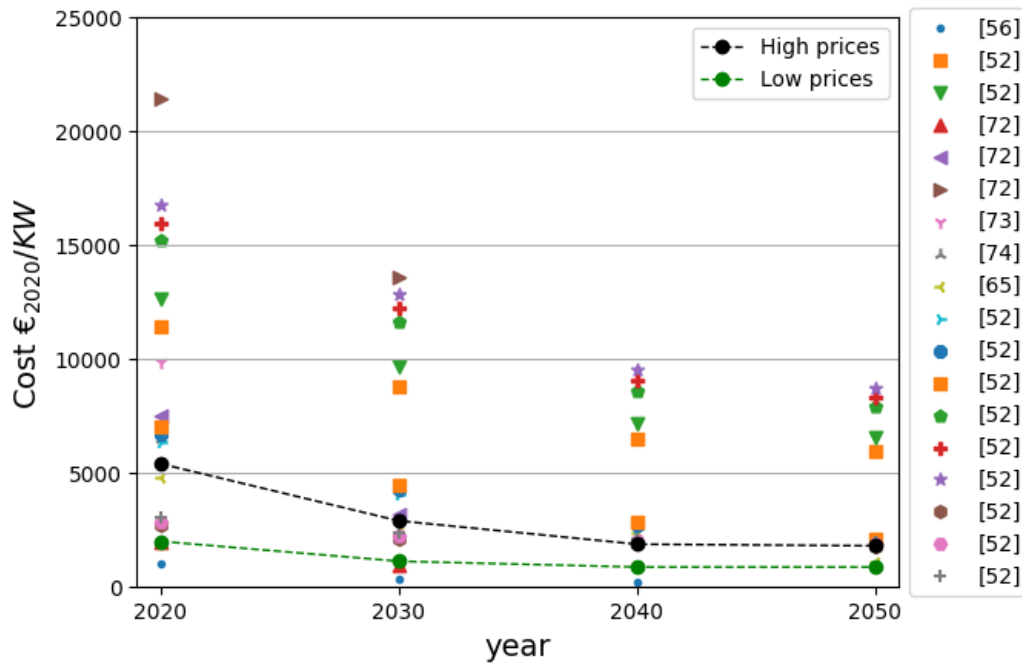


Figure A.3: The fuel cell cost plotted with time. The points in the legend corresponds with the source in the bibliography[52, 56, 65, 72–74].

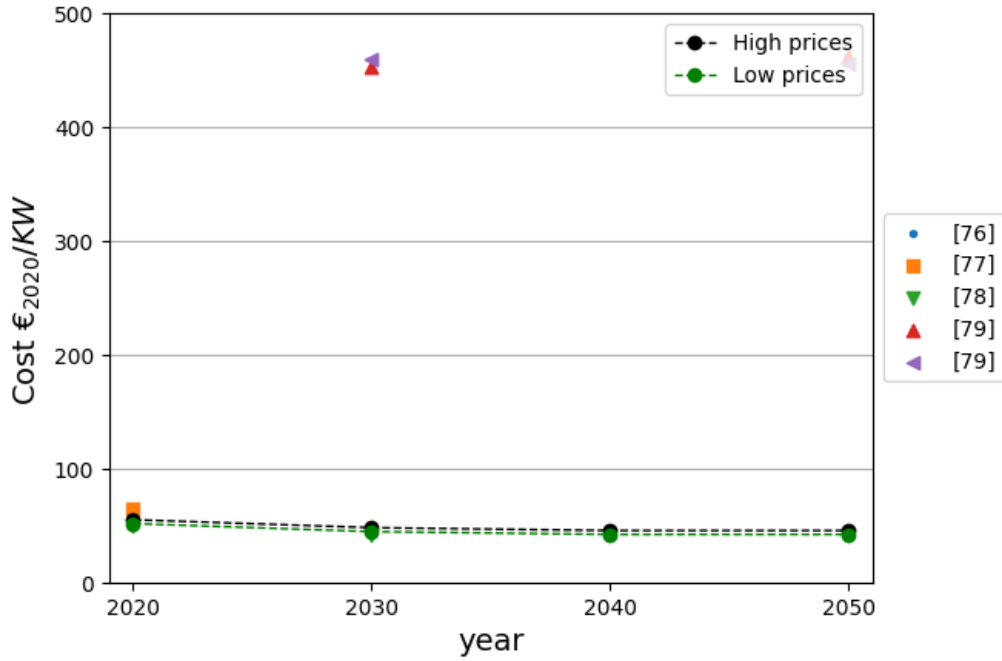


Figure A.4: The cost of a hydrogen boiler plotted with time. To get the boiler unit price for this model the cost has to multiplied by 40. This plot was modified to illustrate the trend lines clearly, the unmodified data points plot can be seen in appendix A figure A.3. The points in the legend corresponds with the source in the bibliography[76–79].

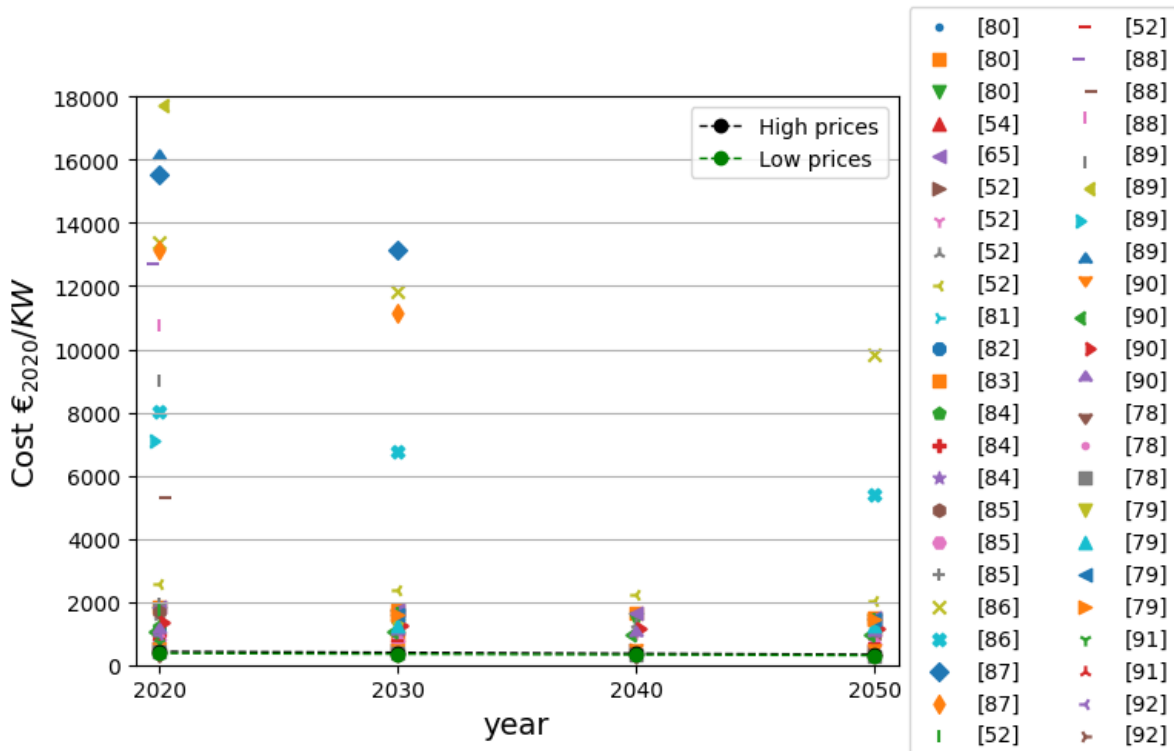


Figure A.5: The heat pump system cost plotted with time. To get the heat pump unit price for this model the cost has to be multiplied by 7.9. The points in the legend corresponds with the source in the bibliography[52, 54, 65, 78, 80–92].

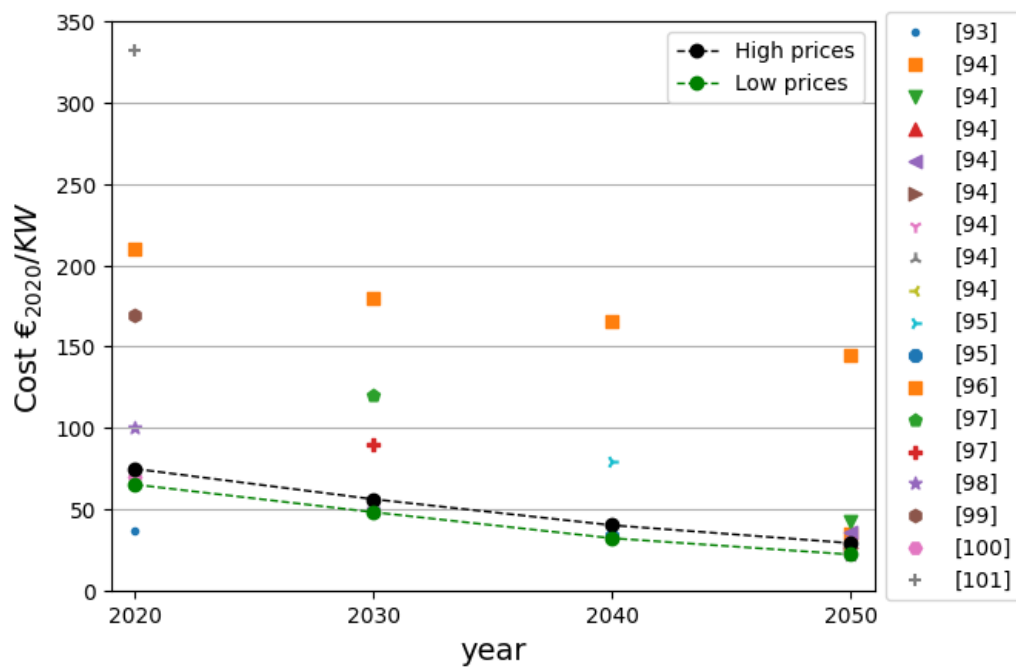


Figure A.6: The inverter unit cost plotted with time. The points in the legend corresponds with the source in the bibliography[93–101].

B

Optimisation results

Here the results of the optimal system size from the optimisation can be seen for all the cases. Also the simulation results can be seen for some particular parameters. First the fully electrical scenario results will be presented followed by the integrated hydrogen scenario.

Table B.1.: The results of the sizing for the hybrid system for each case in the fully electrical neighborhood scenario.

Case	Year	N _{SS}	N _{SWW}	N _{NNW}	N _{NEE}	Park multiplier	Rated power electrolyser [KW]	Rated power fuel cell [KW]	Battery [KWh]	Tank volume [m ³]
C-EBase	2020	12.0	9.0	18.5	19.0	0	720	360	5975	400
	2030	20.0	20.0	13.0	16.0	0	1080	480	1375	500
	2040	20.0	20.0	19.0	20.0	0	1080	480	1275	400
	2050	20.0	20.0	20.0	20.0	0	840	480	1075	400
C-Ev	2020	20.0	20.0	15.0	20.0	0	1140	600	8525	600
	2030	20.0	20.0	15.0	20.0	0	1020	600	8375	550
	2040	19.5	19.0	15.0	20.0	0	900	600	8275	500
	2050	20.0	15.0	19.5	20.0	0	1020	600	6775	550
C-EH	2020	20.0	20.0	20.0	20.0	0	5340	1080	7825	1425
	2030	20.0	20.0	20.0	20.0	0	3540	900	8400	1225
	2040	20.0	20.0	19.5	20.0	0	3060	900	8100	1200
	2050	20.0	20.0	20.0	20.0	0	2340	900	8350	1100
C-Ev+H	2020	20.0	20.0	20.0	20.0	40	9180	1440	11950	1500
	2030	20.0	20.0	20.0	20.0	40	9780	1620	12000	1500
	2040	20.0	20.0	20.0	20.0	40	9360	1560	12000	1500
	2050	20.0	20.0	20.0	20.0	33	8880	1560	12000	1500

Table B.2: The results of some parameters of the hybrid system for each case in the fully electrical neighborhood scenario. These results are related to the low prices components trend.

Case	Year	Energy from the grid [MWh]	Energy to the grid [MWh]	SSR [%]	Energy to system [MWh]	System cost [M€]	Revenue [M€]	LCEO [€/KWh]
C-EBase	2020	33.40	2720.82	0.996	3262.33	20.37	1.83	0.48
	2030	32.69	3774.07	0.917	3479.14	16.68	2.56	0.34
	2040	29.38	5134.18	0.876	3273.67	11.66	3.49	0.25
	2050	29.26	5422.66	0.911	3138.15	9.43	3.69	0.21
C-Ev	2020	47.56	3361.70	0.971	4753.56	29.80	2.26	0.44
	2030	41.29	3731.91	0.878	4563.56	20.88	2.52	0.32
	2040	38.00	3855.08	0.843	4375.72	15.44	2.61	0.25
	2050	36.59	4375.72	0.824	4311.81	16.56	2.29	0.23
C-EH	2020	53.55	1445.73	0.911	5710.37	57.42	0	0.71
	2030	55.02	730.29	0.969	5512.34	40.37	0.43	0.52
	2040	51.59	1015.33	0.936	5358.58	34.64	0.63	0.45
	2050	63.09	1688.57	1.164	5253.60	30.53	1.06	0.40
C-Ev+H	2020	155.48	0.414	2.128	6994.89	70.82	0	0.72
	2030	95.42	0.03	1.327	6943.27	55.73	0	0.57
	2040	81.19	0.01	1.156	6792.05	46.53	0	0.49
	2050	78.14	0.03	1.142	6616.74	42.44	0	0.46

Table B.3: The results of the sizing for the hybrid system for each case in the integrated hydrogen neighborhood scenario.

Case	Year	N _{SSE}	N _{SWW}	N _{NNW}	N _{NPE}	Park multiplier	Rated power electrolyser [KW]	Rated power fuel cell [KW]	Battery [KW/h]	Tank volume [m ³]
C-H ₂ V	2020	20.0	20.0	20.0	20.0	40.0	8600	1080	7950	1500
	2030	20.0	20.0	20.0	20.0	40.0	8600	1080	7950	1500
	2040	20.0	20.0	20.0	20.0	40.0	8600	1080	7950	1500
	2050	20.0	20.0	20.0	20.0	35.0	8600	480	7925	1150
C-H ₂ H	2020	19.5	20.0	12.5	20.0	0	5540	460	9925	850
	2030	19.5	20.0	12.0	19.5	0	4340	400	9450	825
	2040	17.0	18.5	12.0	20.0	0	5060	340	9675	800
	2050	17.0	18.5	11.5	20.0	0	4100	340	9425	700

Table B.4: The results of some parameters of the hybrid system for each case in the fully electrical neighborhood scenario. These results are related to the low prices components trend. For this scenario it was chosen to leave out the results of C-H₂_V and C-H₂_{V+H} as both did not produce any feasible data.

Case	Year	Energy from the grid [MWh]	Energy to the grid [MWh]	SSR _E [%]	SSR _{H₂} [%]	Energy to system [MWh]	System cost [M€]	LCEO [€/KWh]
C-H ₂ H	2020	48.34	0.92	1.198	25.86	3929.77	43.08	0.78
	2030	43.95	111.65	1.13	25.59	3768.77	33.61	0.63
	2040	41.50	45.09	1.12	25.97	3611.50	28.98	0.57
	2050	35.73	574.98	1.03	30.66	3394.54	24.73	0.52

Bibliography

- [1] IEA. *Renewable Energy Market Update 2021*. Tech. rep. IEA, Paris, 2021. URL: <https://www.iea.org/reports/renewable-energy-market-update-2021>.
- [2] *Research*. May 2021. URL: <https://www.fraunhofer.de/en/research.html>.
- [3] *World energy outlook. 2020 / International Energy Agency*. eng. IEA, 2020.
- [4] Nancy M. Haegel et al. “Terawatt-scale photovoltaics: Transform global energy”. In: *Science* 364.6443 (2019), pp. 836–838. ISSN: 0036-8075. DOI: 10.1126/science.aaw1845. eprint: <https://science.sciencemag.org/content/364/6443/836.full.pdf>. URL: <https://science.sciencemag.org/content/364/6443/836>.
- [5] Marta Victoria et al. “Solar photovoltaics is ready to power a sustainable future”. In: *Joule* 5.5 (2021), pp. 1041–1056. ISSN: 2542-4351. DOI: <https://doi.org/10.1016/j.joule.2021.03.005>. URL: <https://www.sciencedirect.com/science/article/pii/S2542435121001008>.
- [6] Michael Penev, Chad Hunter, and Joshua D Eichman. *Energy storage: Days of service sensitivity analysis*. Tech. rep. National Renewable Energy Lab.(NREL), Golden, CO (United States), 2019.
- [7] Kendall Mongird et al. “2020 grid energy storage technology cost and performance assessment”. In: *Energy 2020* (2020).
- [8] O. Schmidt et al. “Future cost and performance of water electrolysis: An expert elicitation study”. In: *International Journal of Hydrogen Energy* 42.52 (2017), pp. 30470–30492. ISSN: 0360-3199. DOI: <https://doi.org/10.1016/j.ijhydene.2017.10.045>. URL: <https://www.sciencedirect.com/science/article/pii/S0360319917339435>.
- [9] Japanese Ministry of Economy Trade and Industry. *Strategic energy plan*. 2014.
- [10] Jeremy Lagorse et al. “Energy cost analysis of a solar-hydrogen hybrid energy system for stand-alone applications”. In: *International journal of hydrogen energy* 33.12 (2008), pp. 2871–2879.
- [11] Anand Singh, Prashant Baredar, and Bhupendra Gupta. “Techno-economic feasibility analysis of hydrogen fuel cell and solar photovoltaic hybrid renewable energy system for academic research building”. In: *Energy Conversion and Management* 145 (2017), pp. 398–414.
- [12] Himadry Shekhar Das et al. “Feasibility analysis of hybrid photovoltaic/battery/fuel cell energy system for an indigenous residence in East Malaysia”. In: *Renewable and Sustainable Energy Reviews* 76 (2017), pp. 1332–1347.
- [13] Chouki Ghenai and Maamar Bettayeb. “Grid-tied solar PV/fuel cell hybrid power system for university building”. In: *Energy Procedia* 159 (2019), pp. 96–103.
- [14] Normazlina Mat Isa et al. “A techno-economic assessment of a combined heat and power photovoltaic/fuel cell/battery energy system in Malaysia hospital”. In: *Energy* 112 (2016), pp. 75–90.
- [15] Mahdi Fasihi and Christian Breyer. “Baseload electricity and hydrogen supply based on hybrid PV-wind power plants”. In: *Journal of Cleaner Production* 243 (2020), p. 118466. ISSN: 0959-6526. DOI: <https://doi.org/10.1016/j.jclepro.2019.118466>. URL: <https://www.sciencedirect.com/science/article/pii/S0959652619333360>.
- [16] *Photovoltaic Materials and Devices*. July 2021. URL: <https://www.tudelft.nl/ewi/over-de-faculteit/afdelingen/electrical-sustainable-energy/photovoltaic-materials-and-devices>.
- [17] Michel Tamarzians. “A techno-economical feasibility study of an optimal stand-alone Solar-Electrolyzer-Battery-FuelCell system for residential utilization”. MA thesis. Delft, the Netherlands: Delft University of Technology, 2019.
- [18] Megan Atkins. “Future Hydrogen Town: Designing a PV-Hydrogen-Battery-FC system for atypical neighbourhood in the Netherlands”. MA thesis. Delft, the Netherlands: Delft University of Technology, 2020.
- [19] e-Media Resources. URL: <http://www.trnsys.com/>.
- [20] URL: http://lab.fs.uni-lj.si/kes/energetski_sistemi/07%20vaja%20-%20TRNSYS-Getting_started.pdf.
- [21] *Nieuwbouw Ackerswoude: in de omgeving van Rotterdam en Den Haag*. Mar. 2021. URL: <https://www.ackerswoude.nl/>.

- [22] *intro - Meteonorm (de)*. URL: <https://meteonorm.com/en/>.
- [23] Arno H. M. Smets et al. *Solar energy: the physics and engineering of photovoltaic conversion, technologies and systems*. UIT Cambridge, 2016.
- [24] *Panasonic HIT Catalogue*. May 2021. URL: https://eu-solar.panasonic.net/cps/rde/xbcr/solar_en/Panasonic_HIT_Catalogue_EN.pdf.
- [25] International Renewable Energy Agency. *Innovation landscape brief: Utility-scale batteries*. IRENA, 2019.
- [26] Emma Raszmann et al. “Modeling stationary lithium-ion batteries for optimization and predictive control”. In: *2017 IEEE Power and Energy Conference at Illinois (PECI) (2017)*, pp. 1–7.
- [27] *Understanding Batteries*. May 2021. URL: <https://www.spiritenergy.co.uk/kb-batteries-understanding-batteries#>.
- [28] GreenHydrogen.dk et al. *Final report HyProvide Large-Scale Alkaline Electrolyser (MW)*. 2016.
- [29] C. Meurer et al. “PHOEBUS—an autonomous supply system with renewable energy: six years of operational experience and advanced concepts”. In: *Solar Energy* 67.1 (1999), pp. 131–138. ISSN: 0038-092X. DOI: [https://doi.org/10.1016/S0038-092X\(00\)00043-8](https://doi.org/10.1016/S0038-092X(00)00043-8). URL: <https://www.sciencedirect.com/science/article/pii/S0038092X00000438>.
- [30] J. C. Amphlett et al. “Performance Modeling of the Ballard Mark IV Solid Polymer Electrolyte Fuel Cell: I. Mechanistic Model Development”. In: *Journal of The Electrochemical Society* 142.1 (Jan. 1995), pp. 1–8. DOI: 10.1149/1.2043866. URL: <https://doi.org/10.1149/1.2043866>.
- [31] A. Goetzberger et al. “The PV/hydrogen/oxygen-system of the self-sufficient solar house Freiburg”. In: *Conference Record of the Twenty Third IEEE Photovoltaic Specialists Conference - 1993 (Cat. No.93CH3283-9) (1993)*, pp. 1152–1158.
- [32] Rix Industries. *Rix 4VX series datasheet*. Tech. rep. Rix Industries, 2021.
- [33] *Product Datablad – Mercuria*. May 2021. URL: <https://tools.remeha.nl/wp-content/uploads/sites/3/2019/12/Productdatablad-Mercuria.pdf>.
- [34] W. Boyson et al. “Performance Model for Grid-Connected Photovoltaic Inverters”. In: 2007.
- [35] *PVI Commercial Inverters*. May 2021. URL: https://www.solectria.com/site/assets/files/2542/pvi_50-100kw_datasheet_december_2016_rev_1.pdf.
- [36] *World energy outlook. 2019 / International Energy Agency*. eng. OECD/IEA, 2019. ISBN: 9789264523272.
- [37] *Load profile generator*. May 2021. URL: <https://www.loadprofilegenerator.de/>.
- [38] E.A.M. Klaassen et al. “A methodology to assess demand response benefits from a system perspective: A Dutch case study”. In: *Utilities Policy* 44 (2017), pp. 25–37. ISSN: 0957-1787. DOI: <https://doi.org/10.1016/j.jup.2016.11.001>. URL: <https://www.sciencedirect.com/science/article/pii/S095717871630176X>.
- [39] Heike Brugger et al. “Energy Efficiency Vision 2050: How will new societal trends influence future energy demand in the European countries?” In: *Energy Policy* 152 (2021), p. 112216.
- [40] *Remeha maakt opnieuw waterstofprimeur mogelijk*. May 2021. URL: <https://tools.remeha.nl/actueel/remeha-maakt-opnieuw-waterstofprimeur-mogelijk/>.
- [41] *Fuels - Higher and Lower Calorific Values*. May 2021. URL: https://www.engineeringtoolbox.com/fuels-higher-calorific-values-d_169.html.
- [42] “Quantitative analysis of a successful public hydrogen station”. In: *International Journal of Hydrogen Energy* 37.17 (2012). 12th CHEC, pp. 12731–12740. ISSN: 0360-3199. DOI: <https://doi.org/10.1016/j.ijhydene.2012.06.008>. URL: <https://www.sciencedirect.com/science/article/pii/S036031991201350X>.
- [43] *Hoeveel rijden personenauto’s?* May 2021. URL: <https://www.cbs.nl/nl-nl/visualisaties/verkeer-en-vervoer/verkeer/verkeersprestaties-personenautos>.
- [44] *Hyundai NEXO*. May 2021. URL: <https://h2.live/en/wasserstoffautos/hyundai-nexo>.
- [45] *Aardgas en elektriciteit, gemiddelde prijzen van eindverbruikers*. May 2021. URL: <https://opendata.cbs.nl/statline/#/CBS/nl/dataset/81309NED/table?fromstatweb>.
- [46] *Overheid bevordert groei zonne-energie*. May 2021. URL: <https://www.rijksoverheid.nl/onderwerpen/duurzame-energie/zonne-energie>.
- [47] “The hydrogen solution?” In: *Nat. Clim. Chang* 10 (2020), pp. 799–801. DOI: <https://doi.org/10.1038/s41558-020-0891-0>. URL: <https://www.nature.com/articles/s41558-020-0891-0#citeas>.
- [48] *7 Ways to Increase Boiler Lifespan*. May 2021. URL: <https://simulationresearch.lbl.gov/G0/>.

- [49] Eric O'Shaughnessy et al. "The impact of policies and business models on income equity in rooftop solar adoption". In: *Nature Energy* 6.1 (2021), pp. 84–91.
- [50] ISE with support of PSE Projects GmbH Fraunhofer Institute for Solar Energy Systems. *PHOTOVOLTAICS REPORT*. Tech. rep. Fraunhofer-Gesellschaft, 2020.
- [51] Johannes N. Mayer et al. *Current and Future Cost of Photovoltaics*. 2015.
- [52] Johan Carlsson et al. "ETRI 2014—Energy Technology Reference Indicator Projections for 2010–2050". In: *European Commission, Joint Research Centre, Institute for Energy and Transport, Luxembourg: Publications Office of the European Union* (2014).
- [53] Deepak Yadav and Rangan Banerjee. "Economic assessment of hydrogen production from solar driven high-temperature steam electrolysis process". In: *Journal of Cleaner Production* 183 (2018), pp. 1131–1155.
- [54] Jussi Ikäheimo et al. "Role of power to liquids and biomass to liquids in a nearly renewable energy system". In: *IET Renewable Power Generation* 13.7 (2019), pp. 1179–1189.
- [55] Manish Ram et al. "Global energy system based on 100% renewable energy—power sector". In: *Lappeenranta University of Technology and Energy Watch Group: Lappeenranta, Finland* (2017).
- [56] Oliver Schmidt et al. "The future cost of electrical energy storage based on experience rates". In: *Nature Energy* 2.8 (2017), pp. 1–8.
- [57] Ioannis Tsiropoulos, Dalius Tarvydas, and Natalia Lebedeva. "Li-ion batteries for mobility and stationary storage applications Scenarios for costs and market growth". In: *Publications Office of the European Union: Luxembourg* (2018), p. 72.
- [58] *Shell sky scenario*. 2018.
- [59] I Renewable, I Renewable IRENA, et al. "Electricity Storage and Renewables: Costs and Markets to 2030". In: (2017).
- [60] Peter Bronski et al. "The economics of grid defection: When and where distributed solar generation plus storage competes with traditional utility service". In: *Rocky Mountain Institute* (2014), pp. 1–73.
- [61] T Brinsmead et al. "Future energy storage trends". In: *CSIRO, Report* (2015).
- [62] N Lebedeva. "Li-ion batteries for mobility and stationary storage applications". In: *Publications Office of the European Union* (2018).
- [63] David Frankel, Sean Kane, and Christer Tryggestad. "The new rules of competition in energy storage". In: *online: mckinsey.com* (2018).
- [64] T Weiß et al. "Life cycle cost reduction and market acceleration for new nearly zero-energy buildings". In: *IOP Conference Series: Earth and Environmental Science*. Vol. 323. 1. IOP Publishing. 2019, p. 012002.
- [65] Sven Teske et al. "Energy [r] evolution—a sustainable world energy outlook 2015". In: (2015).
- [66] Amela Ajanovic and Reinhard Haas. "Prospects and impediments for hydrogen and fuel cell vehicles in the transport sector". In: *International Journal of Hydrogen Energy* 46.16 (2021), pp. 10049–10058.
- [67] Sayed M Saba et al. "The investment costs of electrolysis—A comparison of cost studies from the past 30 years". In: *International journal of hydrogen energy* 43.3 (2018), pp. 1209–1223.
- [68] Element Energy. *Hydrogen supply chain evidence base, 2018*.
- [69] Fuel Cells and Hydrogen Joint Undertaking. "Development of water electrolysis in the European Union". In: *E4tech Sàrl wit Element Energy Ltd* (2014).
- [70] Gunther Glenk and Stefan Reichelstein. "Economics of converting renewable power to hydrogen". In: *Nature Energy* 4.3 (2019), pp. 216–222.
- [71] *ENEFARM (Residential Fuel Cells)*. May 2021. URL: <https://www.itcenex.com/en/business/detail/enefarm/index.html>.
- [72] Iain Staffell and RJ Green. "Estimating future prices for stationary fuel cells with empirically derived experience curves". In: *International Journal of Hydrogen Energy* 34.14 (2009), pp. 5617–5628.
- [73] *GreenHub 2 PRO 5000*. URL: <https://www.fuelcellstore.com/greenhub-2-pro-5000>.
- [74] *GreenHub 2 PRO 2000*. URL: <https://www.fuelcellstore.com/greenhub-2-pro-2000>.
- [75] *Hydrogen Boilers: An Alternative to Gas Central Heating?* May 2021. URL: <https://www.boilerguide.co.uk/articles/hydrogen-boilers-alternative-gas-central-heating>.
- [76] *HRE 36/48 A*. May 2021. URL: <https://www.intergas-verwarming.nl/en/trade/products/hre/hre-36-48-a/>.
- [77] *XTREME 36*. May 2021. URL: <https://www.intergas-verwarming.nl/en/consumer/products/xtreme/xtreme-36/>.

- [78] Paige Jadun et al. *Electrification futures study: End-use electric technology cost and performance projections through 2050*. Tech. rep. National Renewable Energy Lab.(NREL), Golden, CO (United States), 2017.
- [79] D. Connolly et al. “Heat Roadmap Europe: Combining district heating with heat savings to decarbonise the EU energy system”. In: *Energy Policy* 65 (2014), pp. 475–489. ISSN: 0301-4215. DOI: <https://doi.org/10.1016/j.enpol.2013.10.035>. URL: <https://www.sciencedirect.com/science/article/pii/S0301421513010574>.
- [80] Sven Teske. *Achieving the Paris climate agreement goals: global and regional 100% Renewable energy scenarios with non-energy GHG pathways for+ 1.5 C and+ 2 C*. Springer Nature, 2019.
- [81] J Arran and J Slowe. “2050 Pathways for Domestic Heat Final Report”. In: *Delta Energy & Environment Ltd.: Edinburgh, UK* (2012).
- [82] Peter C Slorach and Laurence Stamford. “Net zero in the heating sector: Technological options and environmental sustainability from now to 2050”. In: *Energy Conversion and Management* 230 (2021), p. 113838.
- [83] Robert Sansom. “Decarbonising low grade heat for low carbon future”. PhD thesis. Imperial College London, 2014.
- [84] Robin Niessink. *GROUND SOURCE HEAT PUMP - HOUSEHOLDS*. 2019. URL: <https://energy.nl/wp-content/uploads/2019/05/Technology-Factsheet-Heat-pump-soil-households.pdf>.
- [85] Robin Niessink. *AIR SOURCE HEAT PUMP*. 2019. URL: <https://energy.nl/wp-content/uploads/2019/02/Technology-Factsheet-Heat-pump-air-households-1.pdf>.
- [86] Menkveld et al. *De systeemkosten van warmte voor woningen*. 2015. URL: <https://repository.tno.nl/islandora/object/uuid%5C%3A9d49b1d3-107b-4f49-a36c-b606786bc207>.
- [87] Startmotor. *Calculations Natural gas free dwellings(scenario 98m2)*. 2018.
- [88] Rolf Heynen et al. “Nationaal warmtepomp trendrapport 2018”. In: *Dutch New Energy* (2018).
- [89] *Factsheet bodemwarmtepomp*. 2018.
- [90] Planenergi Fond. “Techno-economic projections until 2050 for smaller heating and cooling technologies in the residential and tertiary sectors in the EU”. In: *Joint Research Centre (European Commission)* (2017).
- [91] Remeha. *Mercuria*. 2021. URL: <https://www.remeha.nl/product/mercuria#productInfoTabber2>.
- [92] Rameha. *Eria Tower*. 2021. URL: <https://www.remeha.nl/product/eria-tower>.
- [93] Marcel Cremers et al. *Conceptadvies SDE++ 2020: verbranding en vergassing van biomassa*. PBL Planbureau voor de Leefomgeving, 2019.
- [94] ISE Fraunhofer and Agora Energiewende. “Current and future cost of photovoltaics. Long-term Scenarios for Market Development, System Prices and LCOE of Utility-Scale PV systems”. In: *Agora Energiewende* 82 (2015).
- [95] Abdulrahman Alassi, Omar Ellabban, and Santiago Bañales. “Generic distributed photovoltaic cost outlook methodology: Australian market application example”. In: *2018 7th International Conference on Renewable Energy Research and Applications (ICRERA)*. IEEE. 2018, pp. 144–149.
- [96] Alo Allik, Heiki Lill, and Andres Annuk. “Effects of Price Developments on Photovoltaic Panel to Inverter Power Ratios”. In: *2019 8th International Conference on Renewable Energy Research and Applications (ICRERA)*. IEEE. 2019, pp. 371–376.
- [97] Jessika E Trancik et al. *Technology improvement and emissions reductions as mutually reinforcing efforts: Observations from the global development of solar and wind energy*. Tech. rep. MIT, 2015.
- [98] Winfried Hoffmann. *The economic competitiveness of renewable energy: pathways to 100% global coverage*. John Wiley & Sons, 2014.
- [99] SolarToday. *SMA Sunny Tripower CORE2 STP110-60*. 2021. URL: <https://www.solartoday.eu/sma/>.
- [100] SolarToday. *SAJ Suntrio Plus 50K, 3MPPT*. 2021. URL: <https://www.solartoday.eu/product/saj-suntrio-plus-50k-3mppt/>.
- [101] Solaris. *SOLECTRIA PVI-75-480 75KW INVERTER*. 2021. URL: <https://www.solaris-shop.com/solectria-pvi-75-480-75kw-inverter/>.
- [102] *GenOpt Generic Optimizatio program*. May 2021. URL: <https://simulationresearch.lbl.gov/GO/>.
- [103] J. Kennedy and R. Eberhart. “Particle swarm optimization”. In: *Proceedings of ICNN'95 - International Conference on Neural Networks*. Vol. 4. 1995, 1942–1948 vol.4. DOI: 10.1109/ICNN.1995.488968.

- [104] Michael Wetter. *GenOpt Generic Optimization Program User Manual Version 2.1.0*. English. Version 2.1.0. Lawrence Berkeley National Laboratory. 109 pp.
- [105] Robert Hooke and Terry A Jeeves. ““Direct Search”Solution of Numerical and Statistical Problems”. In: *Journal of the ACM (JACM)* 8.2 (1961), pp. 212–229.
- [106] Jörn Brauns and Thomas Turek. “Alkaline Water Electrolysis Powered by Renewable Energy: A Review”. In: *Processes* 8.2 (2020). ISSN: 2227-9717. DOI: 10.3390/pr8020248. URL: <https://www.mdpi.com/2227-9717/8/2/248>.
- [107] Emanuele Taibi et al. “Green Hydrogen Cost Reduction”. In: (2020).
- [108] US Department of Energy. *Hydrogen Fuel Cells*. URL: https://www.californiahydrogen.org/wp-content/uploads/files/doe_fuelcell_factsheet.pdf.
- [109] Matthew A Pellow et al. “Hydrogen or batteries for grid storage? A net energy analysis”. In: *Energy & Environmental Science* 8.7 (2015), pp. 1938–1952.